# System Demonstrator of a Portable NIR Spectrometer for Rapid Stone Dust Compliance Testing

## Milestone Three Report

Simtars

## Report Information

**Title:** *System Demonstrator of a Portable NIR Spectrometer for Rapid Stone Dust Compliance Testing*

**Client:** *Lynne Magee*
*Project Liaison Officer*
*Coal Health and Safety Trust*
*Level 21*
*44 Market Street*
*GPO Box 2842*
*Sydney*
*NSW 2000*
*Australia*

**Client Reference:** *20663*

**Document No:** *MR303-0014-0003*

## Author, Reviewer and Approver Details

| | | | | |
|---|---|---|---|---|
| **Prepared by:** | Shevaune Zeng<br>Senior Engineer | **Date:** | 12/01/2024 |  |
| **Reviewed by:** | Eleonora Widzyk-Capehart<br>Principal Scientist | **Date:** | 12/01/2024 |  |
| **Approved by:** | Gareth Kennedy<br>Director MSTRC | **Date:** | 12/01/2024 |  |

## Document Owner

State of Queensland as represented by Resources Safety & Health Queensland (RSHQ) acting through the Safety in Mines, Testing and Research Station (Simtars)

ABN 49 809 734 894

2 Robert Smith Street, Redbank, Queensland, Australia 4300

169 Sydney Street, Mackay, Queensland, Australia 4740

Tel: +61 7 3810 6333

Fax: +61 7 3810 6363

Email: enquiries@simtars.com.au

www.simtars.com.au

Certified to ISO 9001, ISO 14001, AS/NZS 4801, ISO/IEC 17025:2005

Registered Training Organisation (National Provider Number 45647)

# Contents

# Table of Figures

# Table of Tables

# Executive Summary

This milestone report No. MR303-0014-0003 is a final report, summarising the comprehensive work regime and analysis undertaken for the Coal Health and Safety Trust Project 20663 entitled “System Demonstrator of a Portable NIR Spectrometer for Rapid Stone Dust Compliance Testing”.

This project sought to demonstrate that the currently commercially available devices can be used to determine the total incombustible content (TIC).

This report provides the performance evaluation of two portable spectrometers, Stellarnet NIR ADK and Lightnovo miniRaman, with respect to: sample preparation, model development, and their abilities to predict TIC.

The spectrometers’ performance was evaluated based on randomly selected one hundred coal samples from Queensland and New South Wales, each of them dosed with three varying amounts of stone dust, producing 300 coal/stone dust samples. Cross-validation during sample preparation for TIC analysis was completed by Simtars internal laboratory and Coal Services NSW external laboratory, indicating systematic error within sample preparation. Consequently, internal laboratory TIC values were utilized in the data analysis.

The application of the Stellarnet NIR ADK portable spectrometer yielded the most favourable predictive performance in rapid TIC analysis, notably through the development of the NIR Linear Regression Model. The NIR Linear Regression Model exhibited superior predictive performance, achieving RMSE of 2.87 % and $R^2$ of 0.81, which aligned closely with the project objectives of RMSE ≤ 5 % and $R^2$ ≥ 0.8.

The evaluation of the Lightnovo miniRaman portable spectrometer delivered less optimal predictive performance in real-time stone dust analysis to-date than the Stellarnet NIR spectrometer. The overall results might have been affected by various factors ranging from data acquisition, model training and the time constraints, which limited the scope of the evaluation, as compared to the Stellarnet NIR ADK spectrometer. Further analysis is warranted as recent studies related to coal samples suggest that additional Raman spectra acquired with various laser power setting and a systematic deconvolution process of the Raman spectra data would attain favourable results.

# 1.0 Introduction

This report No. MR303-0014-0003 for the Coal Services Project 20663 entitled “System Demonstrator of a Portable NIR Spectrometer for Rapid Stone Dust Compliance Testing” is the final report comprehensively addressing the objectives and outcomes of the project across the following sections:

Section 2.0: Project Overview

Section 3.0: Spectrometer Selection

Section 4.0: Sample Preparation

Section 5.0: Model Development for Stellarnet NIR ADK Portable Spectrometer

Section 6.0: Model Development for Lightnovo miniRaman Portable Spectrometer

Section 7.0: NIR and Raman Model Comparison

Section 8.0: Conclusions

Section 9.0: Recommendations and Future Developments

The first milestone report, issued on the 5th of June 2023, provided the project overview, detailed the sample selection, preparation and analysis, summarised the spectrometer selection and its early evaluation, and outlined the testing workflow and machine learning methodology (see Report No. MR303-0014-0001).

The second milestone report, issued on the 6th of October 2023, updated the project budget, detailed the validation of sample preparation, provided the preliminary data pre-processing and machine learning outcomes for StellarNet NIR ADK portable spectrometer, and updated the timeline for the Lightnovo miniRaman portable spectrometer (see Report No. MR303-0014-0002).

# 2.0 Project Overview

## 2.1. Background

Australian Coal mines are subject to a range of hazardous conditions that could prove costly to human life, especially coal dust explosions. To mitigate these risks, regulations, such as Recognised Standard 5 (RS5) (Resources Safety and Health Queensland, 2023), mandate the dilution of combustible dust in the mine environment with limestone dust. This process renders the dust inert in the presence of an ignition source, based on insights gained from past incidents and lessons learned.

In the USA, the Coal Dust Explosibility Meter (CDEM) was developed by NIOSH for rapid evaluation. The device uses a photodiode to evaluate the concentration of total incombustibles present in a sample. The device was evaluated in the field for use in Australian coal mines (Wedel, et al., 2015). However, a few shortcomings were identified, leading to the recommendation against its immediate adoption in the Australian context. These drawbacks encompassed inadequate reference sample design for Australian coal mines, user-unfriendly calibration methodology, and a lack of certification for intrinsic safety. Furthermore, the operational principle of the test rendered it sensitive to moisture within the sample, necessitating the pre-testing drying of samples.

While the current methodology for assessing stone dust compliance relies on colorimetric testing for on-the-spot evaluation, this approach has its own set of limitations in terms of precision and sensitivity as it may be influenced by factors, such as, lighting conditions and operator subjectivity (Wedel, et al., 2015).

## 2.2. Total Incombustible Content

For Queensland, Australia, RS5 stipulates the requirements for incombustible content per zone, and how the testing methodologies are to be conducted. RS5 allows a portable instrument to be used for the analysis of roadway dust samples if it is as accurate as laboratory analysis. However, RS5 does not stipulate the accuracy required for laboratories undertaking analysis.

Within NSW, Australia, *"Roadway Dust Analysis in Underground Coal Mines"* provides the stipulations for analysis of roadway dust for underground coal mines (NSW Resources Regulator, 2015). Similar to RS5, in this NSW Standard, the "chemical" method (laboratory) is deemed the authoritative method, however, no minimum laboratory accuracy is stipulated. Additionally, there is no stipulation for portable instrumentation in the NSW Standard.

A comparison of the reported rates of uncertainty (unexpanded) for each laboratory and the CDEM is provided in Table 1.

***Table 1 Uncertainty of Analysis for Incombustible Content by Laboratory and Instrument***

| Source | Uncertainty of Analysis | Procedure |
|---|---|---|
| Simtars (QLD) | ± 25 % (Simtars, 2022) | Procedure for Determination of the Incombustible Content of Roadway Dust – LP0012 (Simtars, 2022) |
| Coal Services (NSW) | ± 0.1 % (Coal Services, 2023) | Roadway Dust Analysis in Underground Coal Mines and In-house TM017 (NSW Resources Regulator, 2015) |
| MSHA – National Air and Dust Laboratory (USA) | ± 0.7 %[1] | Low Temperature Ashing (LTA) Method (Sapko, et al., n.d.) |
| CDEM | ± 2 %[2] (Schauenburg, 2023) | N/A |

Additionally, Report IC 9529 states that an interlaboratory comparison undertaken within USA showed a 1.7 % variation in standard deviation for well-prepared samples and can increase to 7 % incombustible content variation if samples were not adequately mixed/subdivided (Harris, et al., 2012).

Laboratory gravimetric analysis is not a true measurement for material incombustibility. The only direct measurement of explosibility is by using a 20 L sphere or other combustible dust explosion apparatuses. Therefore, both gravimetric and spectral measurements of roadway dusts are testing for incombustibility by inference.

The provision for instrumentation to be used in place of laboratory methodology requires that instrumentation is as accurate as laboratory methodology. This poses a challenge with how accuracy is reported not only between laboratories, but also due to the fundamental differences of the tests (gravimetric vs spectrometry). For instance, the CDEM provides a qualitative result (Go/No Go) while the laboratory testing provides a quantitative analysis. While CDEM will allow a direct comparison with spectroscopy classification models, regression models will need to be inferred.

In addition, the specification sheet for the CDEM states that the accuracy is ± 2 % (Schauenburg, 2023), however, this is only true when using completely dried samples. Report IC 9529 states that 1 % moisture can decrease the IC readings by as much as 7 %. Additionally, this accuracy may be for classification cut-off and thus, most likely does not provide a direct incombustible content.

[1] The MSHA reported value of ± 0.7 % is unclear if it is an uncertainty of analysis or the error of measurement with a reference standard.

[2] The value reported appears to only pertain to the Pass/Fail at 80 % total incombustible.

## 2.3. Spectrometers

The existing CDEM developed by NIOSH can provide real-time incombustible content analysis. It operates using broadband infrared (IR) sensors. However, a study published at the Resource Operators Conference (Wedel, et al., 2015) provided an analysis of the overall performance of the system. It found that the device was not recommended for adoption for use in Australian mining due to a few key disadvantages. Primarily, the device could not detect past 80 % due to the calibration model built in, and it was affected by inherent sample moisture. Additionally, the CDEM only provides a PASS / FAIL result, not a concentration analysis.

The rapid development of spectral sensors within the last decade has resulted in numerous portable spectrometers being developed and available on the market. This has allowed for the identification of materials in the field rather than the laboratory. More recently, advances in regression modelling along with higher resolution sensors now allow for portable quantitative analysis of materials. For instance, portable X-ray fluorescence has been used for the analysis of ash content in coal (Ching, 2017).

## 2.4. Project Objectives

The ultimate goal is to develop a prototype demonstrator unit for rapid stone dust analysis with an easy-to-use interface that automatically calculates total incombustibles of the analysed samples. This project sought to demonstrate that the currently commercially available devices can be used to determine the total incombustible content.

The aims of this project were defined as follows:

1. Select a ready-to-use portable spectrometer with the following specifications:
    a. Costs of no more than $25,000 AUD per unit.
    b. Minimal to zero development time/cost to allow analysis to be undertaken immediately.
    c. Minimal lead time for acquisition.
    d. Does not contain or require components that would exclude it from hazardous areas, e.g., high voltage photomultipliers and Class 4 lasers.
2. Prepare a range of representative coal/stone dust samples with three normal distributions that could likely be found with roadway dusts for TIC of:
    a. 70 %
    b. 80 %
    c. 85 %
3. Develop regression and classification models, either with standard regression analysis or machine learning, that can predict the incombustible content of samples meeting the following requirements:
    a. For Regression Model:
        i. Root Mean Square Error (RMSE) of ≤ 5 %
        ii. $R^2$ of ≥ 0.8 (if applicable to the model)
    b. For Classification Model:
        i. Confusion Matrix better than the CDEM provided by Wedel et al (2015) (Figure 1)

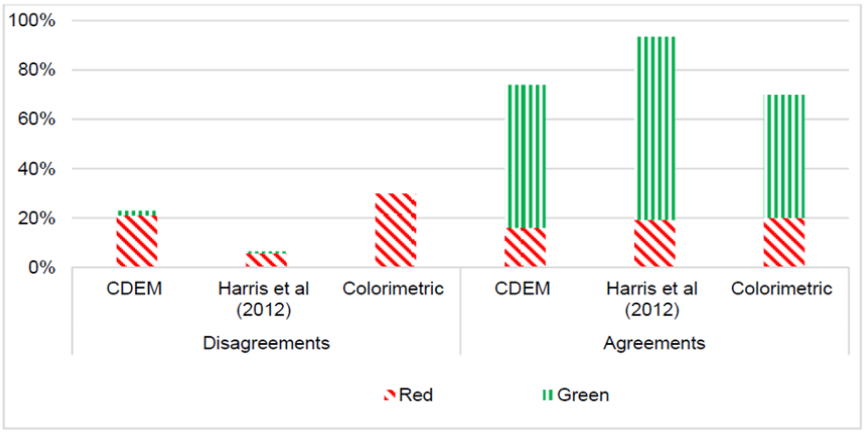


***Figure 1 Average Disagreements and Agreements between CDEM, Harris et al., (2012) and Colorimetric Results with LTA for 80 % TIC*** *(Wedel, et al., 2015)*

At the end of the project, a system demonstrator was to be developed that would affirm the viability of a portable NIR spectrometer device for rapid stone dust compliance testing in Australian coal mines.

## 2.5. Timeline

The project commenced in January 2023, with a final spectrometer review undertaken to ensure that no new systems were available on the market compared to earlier analysis. The review resulted in the selection of two spectrometers: Stellarnet NIR ADK portable spectrometer, which arrived in late April 2023, and Lightnovo miniRaman portable spectrometer, which arrived in late July 2023.

The sample selection and preparation commenced in March 2023, and the last stage of the sample preparation was finalised in early April 2023.

The comprehensive scanning of NIR spectra using the Stellarnet NIR ADK portable spectrometer was completed in May 2023. Preliminary pre-processing, analysis, and model development of NIR data were presented in the second milestone report in October 2023, while the final and improved results are detailed in this final milestone report in January 2024, as per schedule.

The complete Raman spectra scanning utilizing the Lightnovo miniRaman portable spectrometer was finalised in December 2023. The pre-processing, analysis, and model development for Raman data are outlined in the final milestone report in January 2024.

## 2.6. Budget

The estimated total cost of the project was at $85,921.00. The cumulative project cost, inclusive of labour, reached $97,708.00 AUD ex GST, with the Coal Health and Safety Trust contributing $59,911. The majority of the project cost, totalling $44,158.00, was allocated to the purchase of the two spectrometers. The remaining cost of the project was associated with labour expenses for activities described in Sections 4.0 to 6.0. A detailed breakdown of the costs can be found in Appendix 12.2.

# 3.0 Spectrometer Selection

This project sought to demonstrate that the currently commercially available devices can be used to determine the total incombustible content.

## 3.1. Selection Criteria

The criteria for spectrometer selection were the following:

### 3.1.1. Price

The overall price of the spectrometer of under $25,000 (including the development kit) was deemed reasonable to allow the determination if the sensors can deliver on performance.

### 3.1.2. Ease of Adaptability

The overall user friendliness and configurability of the system were an important criterion as it was not feasible to build a new device within the budget and timeframe allocated.

By using devices specifically made for development, Simtars evaluated the existing technologies, the effectiveness of the algorithms utilised to allocate funding more effectively towards the selected product. Additionally, the devices selected were evaluated for use within an underground coal mining environment. This automatically excluded devices that rely on high energy components, such as, X-Ray Fluorescence, Gamma and Laser Induced Breakdown Spectroscopy.

### 3.1.3. Performance

While pricing and ease of development were prioritised, it was expected that performance might be sacrificed. However, literature has provided substantial evidence that the analysis to be conducted with NIR would not likely require the use of highly sensitive sensors. The reasoning behind this was twofold: firstly, that the overall complexity of the spectra decreases as the total incombustible content increases and, secondly, the utilisation of machine learning for the algorithm reduces the spectra to several primary components across the entire range.

## 3.2. Selected Spectrometers

### 3.2.1. Stellarnet NIR ADK Portable Spectrometer

The Stellarnet NIR ADK portable spectrometer (see Figure 2) provided a few key features that were advantageous to the project: operation within the wavelength range of 900 – 1,700 nm using a crossed Czerny Turner optical system, with < 5 nm resolution and < 0.25 nm wavelength accuracy.

The system was provided in an already operable, ruggedised package, and came with a complete development package to allow greater developmental control of the system. Additionally, the spectrometer has packages that integrate into machine learning systems used by the project, specifically Python and MATLAB drivers. The manufacturer of this device also provided a preliminary analysis of a rudimentary sample, and the results suggested that this model would be an ideal candidate for use.

### 3.2.2. Lightnovo miniRaman Portable Spectrometer

The Lightnovo miniRaman portable spectrometer (see Figure 3) is based on Raman scattering of light. While not truly a near-infrared spectrometer in the traditional sense, it still operates using a near infrared laser. However, research indicated that this method of analysis could be used for coal quality analysis and might have had an advantage for future development towards intrinsically safe design.

The purchased Lightnovo miniRaman portable spectrometer was ready to use without any additional development required by the user meeting the requirement for rapid development with the cost of the device within the price bracket of under $25,000.

*Figure 2 Stellarnet NIR ADK Portable Spectrometer*


*Figure 3 Lightnovo miniRaman Portable Spectrometer*

## 3.3. Rejected Spectrometers

Several instruments were rejected from the initial proposal either due to price, lead time, performance and/or complexity of set-up. These instruments are listed in Appendix 12.1.

# 4.0 Sample Preparation

## 4.1. Sample Selection

For the evaluation of the spectrometers purchased, 100 coal samples from Queensland and New South Wales were randomly selected for analysis. The selected samples were from a range of fresh and aged samples with varying ash and moisture contents to provide diverse and representative spectra.

Prior to sample preparation, these 100 coal samples underwent proximate analysis. Proximate analysis for all selected coal samples was undertaken by ALS Pty Ltd. The spread of values from the proximate analysis are shown in Figure 4.

Additionally, statistical analysis of the coal quality between regions was undertaken to provide a summary of the spread between groups (QLD and NSW) (Table 2).

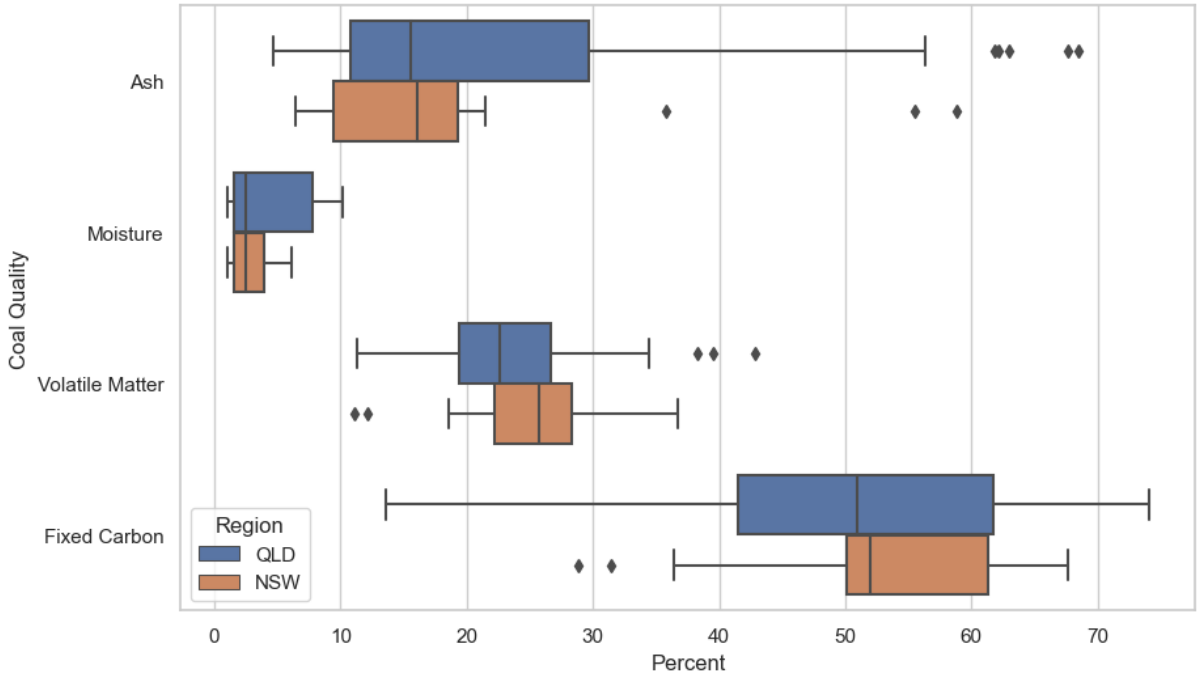


***Figure 4 Coal Quality by Region***

***Table 2 Statistical Analysis of Coal Quality by Region***

| Coal Quality | Levene Test | One-Way ANOVA |
|---|---|---|
| Ash | 0.21, p=0.65 | 0.19, p=0.67 |
| Moisture | 7.20, p=0.009 | 4.60, p=0.04 |
| Volatile Matter | 0.01, p=0.93 | 1.41, p=0.24 |
| Fixed Carbon | 2.32, p=0.13 | 0.16, p=0.69 |

As presented in Figure 4, some coal samples exhibited remarkably high ash contents, reaching approximately 70 %. At the sample preparation stage, it was unknown how the high ash content coal samples might affect the NIR and Raman spectrometer readings. The low moisture content of the coal samples, particularly the NSW coal samples, was likely a result of moisture loss from sample storage

in freezer and the age of the coal samples, which needed to be considered further in terms of the effect on the spectra reading and model development.

As summarized in Table 2, both the Levene Test and the One-Way ANOVA yielded low test statistics and high p-values for all coal quality parameters, except for moisture. Specifically, the p-values for coal quality except for moisture were consistently greater than 0.05, indicating no statistically significant variance among regions (Kasbekar, et al., 2023). This suggests that the 100 coal samples were drawn from similar sample groups across Queensland and New South Wales. The notable difference observed in moisture content between the two regions, as indicated by a p-value less than 0.05, might be attributed to the preservation of the coal samples, considering that these coal samples originated from a span of 20 years.

## 4.2. Sample Dosing

The stone dust dosing regime was determined using three normal distributions centred around regulatory limits of 70 %, 80 %, and 85 %, each with a standard deviation of 5 %. Each of these three normal distributions generated 100 random numbers, which were then randomly applied to the 100 coal samples, resulting in a total of 300 coal/stone dust samples with varying target total incombustible content (TIC) values from the three normal distributions. The spread of the nominated TIC in coal/stone dust samples is displayed in Figure 5, suggesting no significant differences between QLD and NSW regions.

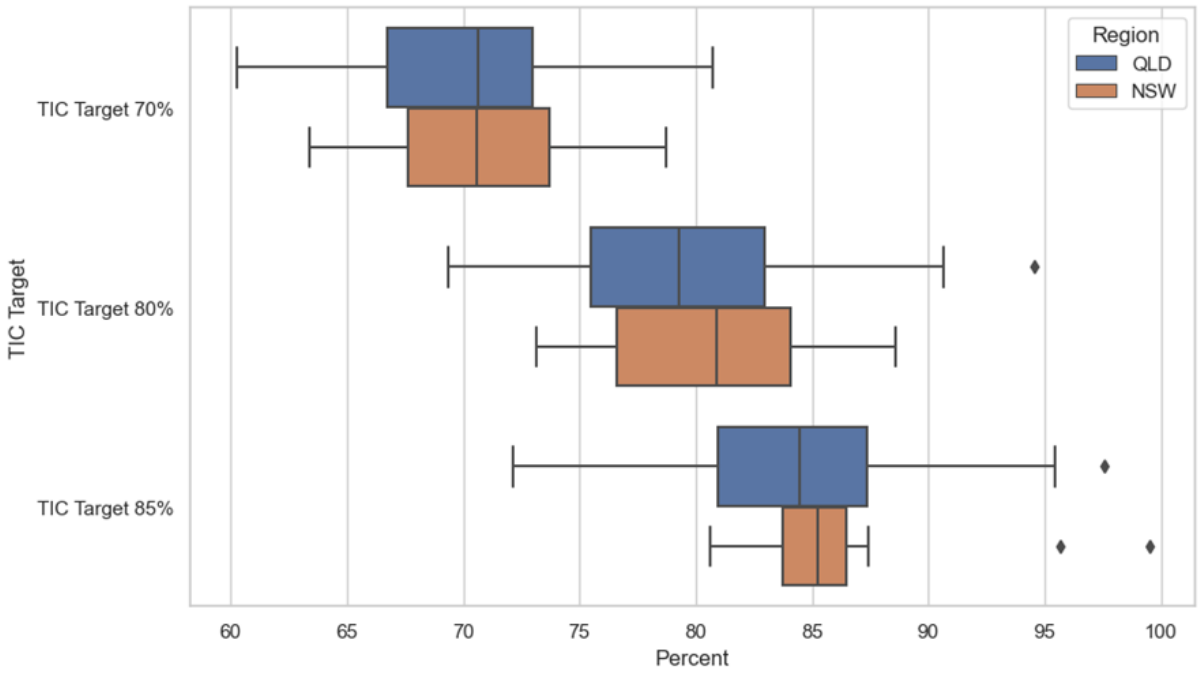


***Figure 5 TIC Target by Region***

The stone dust used for sample preparation was supplied by Sibelco and SEQ Lime. It was not anticipated that different stone dust suppliers would affect the NIR spectra as the primary component, calcium carbonate ($CaCO_3$), does not have strong NIR attenuation.

## 4.3. TIC Validation

Validation of the target stone dust dosing rates was conducted with sub-samples taken from all 300 dosed coal/stone dust samples being tested by Simtars for their TIC. This ensured that the tested coal/stone dust samples were compared to both target TIC values and internal laboratory TIC measurements for potential sources of error.

The comparison between target TIC values and those obtained through Simtars internal laboratory testing is presented in Figure 6, which shows that the internal laboratory values are consistently higher than the target TIC values and that their difference tends to diminish as the target TIC values increase. This systematic pattern of difference indicates the presence of consistent errors within sample preparation, which might be attributable to factors, such as, sample preparation methodologies or equipment precision.

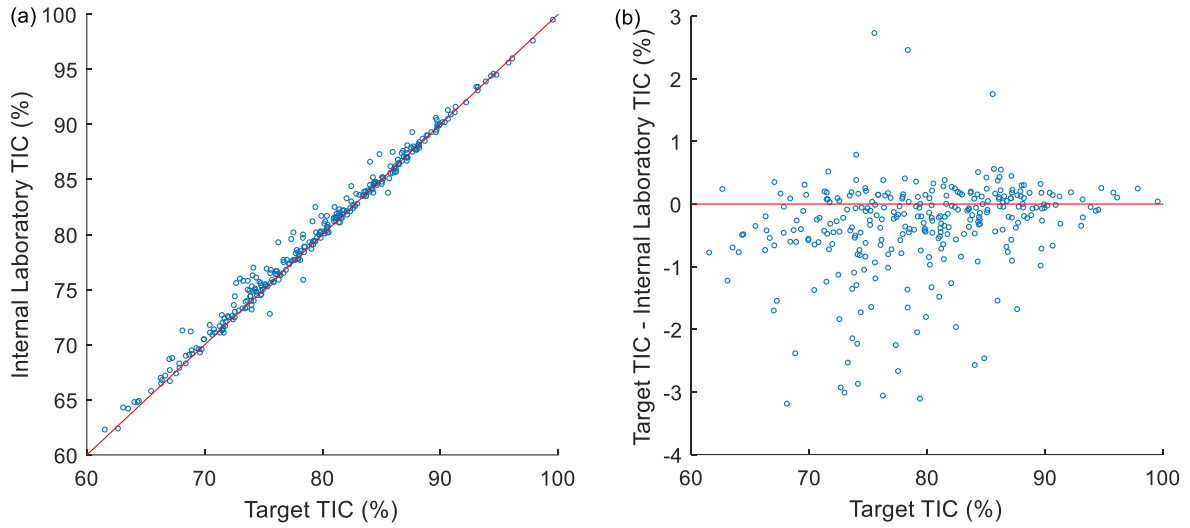


***Figure 6 (a) Target vs. Internal Laboratory TIC; (b) Target TIC vs Difference between Target and Internal Laboratory TIC***

To verify this consistent difference and ensure the accuracy of the results, cross-validation was conducted by randomly selecting 10 sub-samples of the coal/stone dust samples and having them tested by an external laboratory – Coal Services NSW, which followed the same incombustible content analysis methods as Simtars (Simtars, 2022; NSW Resources Regulator, 2015). This cross-validation step helped to verify the accuracy and reliability of the internal laboratory results by comparing the test results obtained at different testing facilities. The results of cross-validation are presented in Figure 7, suggesting that both internal and external laboratory TIC values are higher than target TIC, and that internal and external laboratory measurements follow a tight diagonal trending with an $R^2$ of 0.98 and root mean square error (RMSE) of 0.67 %. Therefore, with a systematic error in target TIC values, the internal laboratory TIC values were used as the actual values in the subsequent machine learning data processing. This approach allowed to maintain the integrity and consistency of the analytical process while addressing potential sources of error.

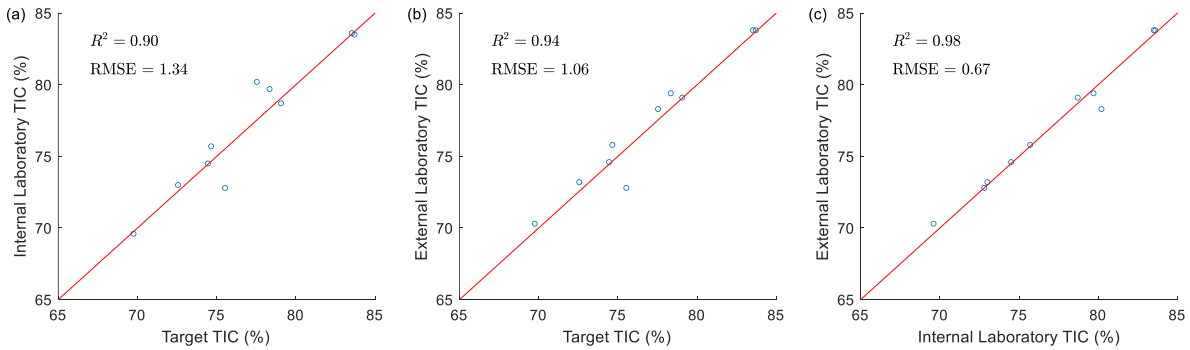


***Figure 7 Comparison of Target, Internal and External Laboratory TIC***

# 5.0 Model Development for Stellarnet NIR ADK Portable Spectrometer

## 5.1. NIR Spectra Data Acquisition

NIR spectra data acquisition commenced with sample scanning using the StellarNet NIR ADK portable spectrometer. A total of 400 samples were scanned for analysis: 100 coal samples and 300 coal/stone dust samples.

NIR spectra data recording was undertaken using the instrument interface as this capability was available within the purchased unit, allowing significant resource savings compared to programming the functionality in-house. The spectral counts and absorbance unit data were saved independently with a unique identifier for each scan.

All the samples subjected to scanning were systematically categorized into five distinct groups, as summarized in Table 3. The raw NIR spectra of the scanned samples are presented in Figure 8.

***Table 3 Categories of Coal and Coal/Stone Dust Samples***

| Category | Actual TIC | Number of Samples |
|---|---|---|
| 1 | < 70 % | 28 |
| 2 | 70 % - 80 % | 116 |
| 3 | 80 % - 85 % | 78 |
| 4 | > 85 % | 78 |
| Coal | Original Coal | 100 |

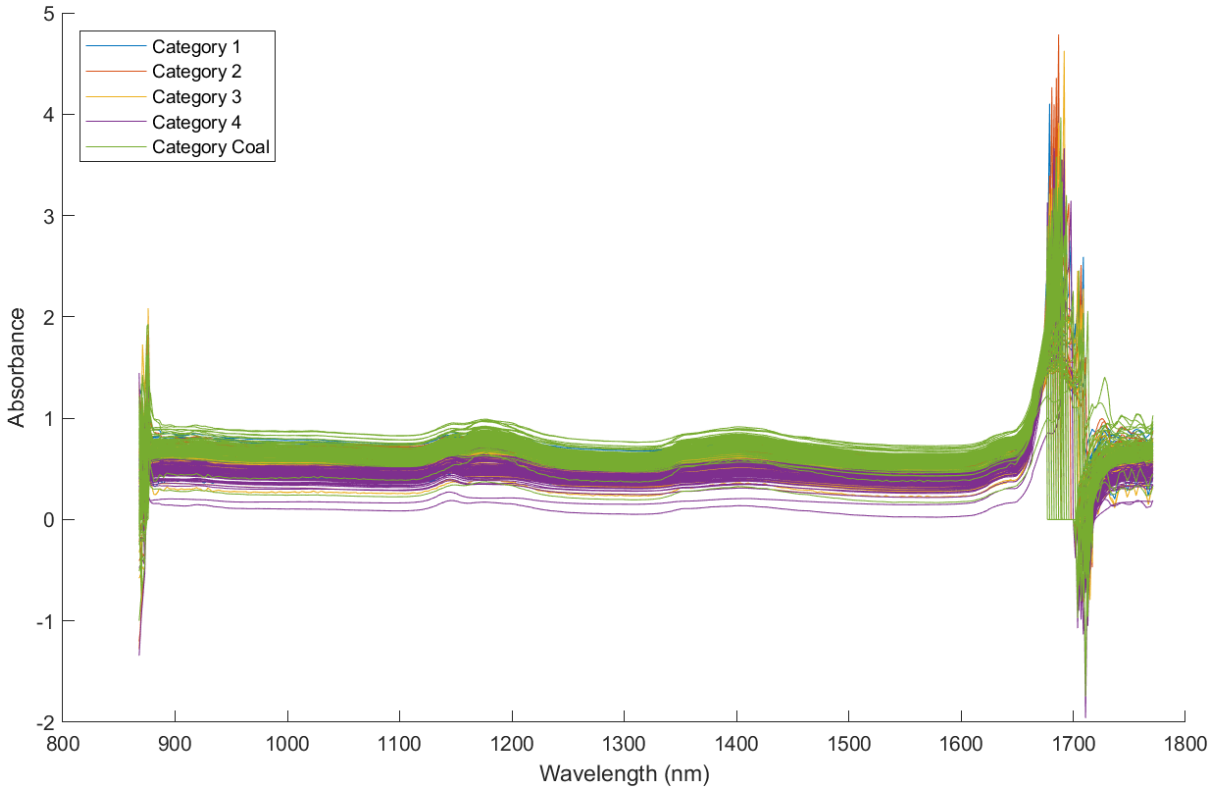


***Figure 8 Raw NIR Spectra***

## 5.2. NIR Spectra Data Pre-Processing

NIR spectra data pre-processing and cleaning were undertaken on the raw NIR spectra of the 300 coal/stone dust samples using a combination of MATLAB and Python, to prepare the data for subsequent machine learning process. The raw NIR spectra of the 100 coal samples were removed as they were not used for model development.

The NIR spectra data pre-processing and cleaning process included:

### 5.2.1. Adjustment of Wavelength Range of Raw NIR Spectra

The raw NIR spectra were truncated to cover the range from 900 nm to 1650 nm due to the noticeable presence of noise in regions below 800 nm and above 1800 nm. The presence of noise aligns with the known limitations of the Stellarnet NIR ADK portable spectrometer's performance in those wavelength extremes. Figure 9 illustrates the truncated NIR spectra with coal samples removed.

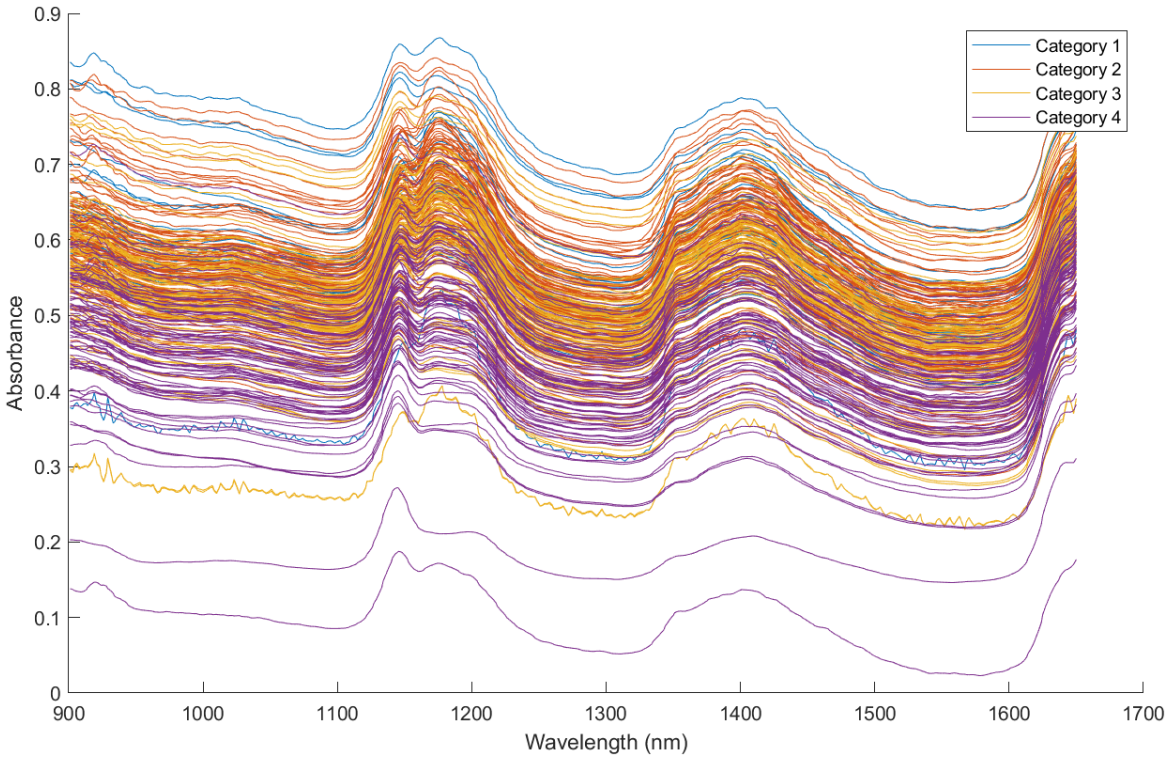


***Figure 9 Truncated NIR Spectra***

### 5.2.2. Correction of Truncated NIR Spectra

The truncated NIR spectra contain unwanted variations caused by factors, such as, sample inhomogeneity, instrument drift, or scattering effects. To enhance the reliability and interpretability of the data, correction techniques were applied to mitigate these variations and improve the quality of the spectra. Among the available correction methods, Standard Normal Variate (SNV) stands out as a popular and effective technique for NIR spectra data. Therefore, SNV was chosen for its ability to reduce baseline shifts and multiplicative effects in the NIR spectra data, enhancing the signal-to-noise ratio and aiding in the extraction of meaningful information (Brown, et al., 2009).

The SNV correction process involved two key steps: centring and scaling. First, each spectrum was centred by subtracting the mean spectrum value from every data point, effectively eliminating baseline shifts and ensuring that the spectrum was centred around zero. Next, the centred spectrum was scaled by dividing each data point by the standard deviation of the spectrum. Scaling normalized the amplitude of the spectrum, correcting for multiplicative effects and making the spectra directly comparable (Brown, et al., 2009). Figure 10 illustrates the NIR spectra after the application of SNV correction.

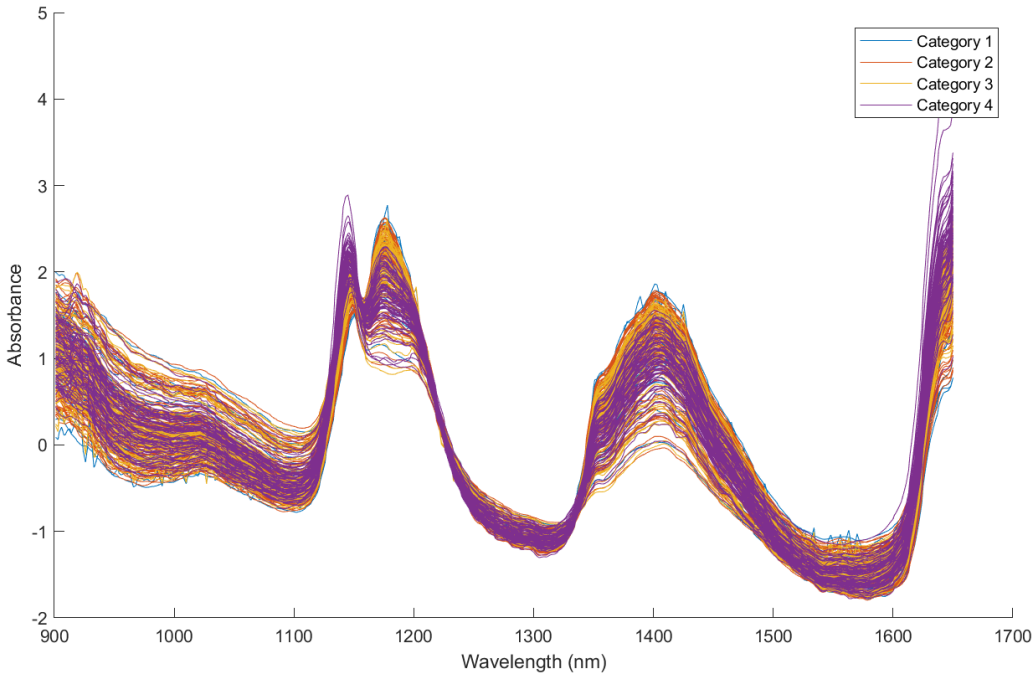


***Figure 10 Corrected NIR Spectra***

### 5.2.3. Smoothing of Corrected NIR Spectra

Spectral smoothing was employed as a pre-processing step to prepare the NIR spectra data for subsequent machine learning process. In this process, various smoothing filters were considered, with the Savitzky-Golay filter being the most commonly used. However, recent research in the field of spectral smoothing has revealed that there were superior methods available, one of which was the Whittaker-Henderson smoother for spectral data (Schmid, et al., 2022).

The Whittaker-Henderson smoother parameter tuning process, which was based on extensive experimentation and analysis, aiming to optimize the spectral smoothing process, revealed that a Whittaker penalty value of 100 provided the best balance between achieving smoothness in the NIR spectra data and retaining important spectral features. Figure 11 provides a graphical illustration of the NIR spectra after applying the Whittaker-Henderson smoothing technique.

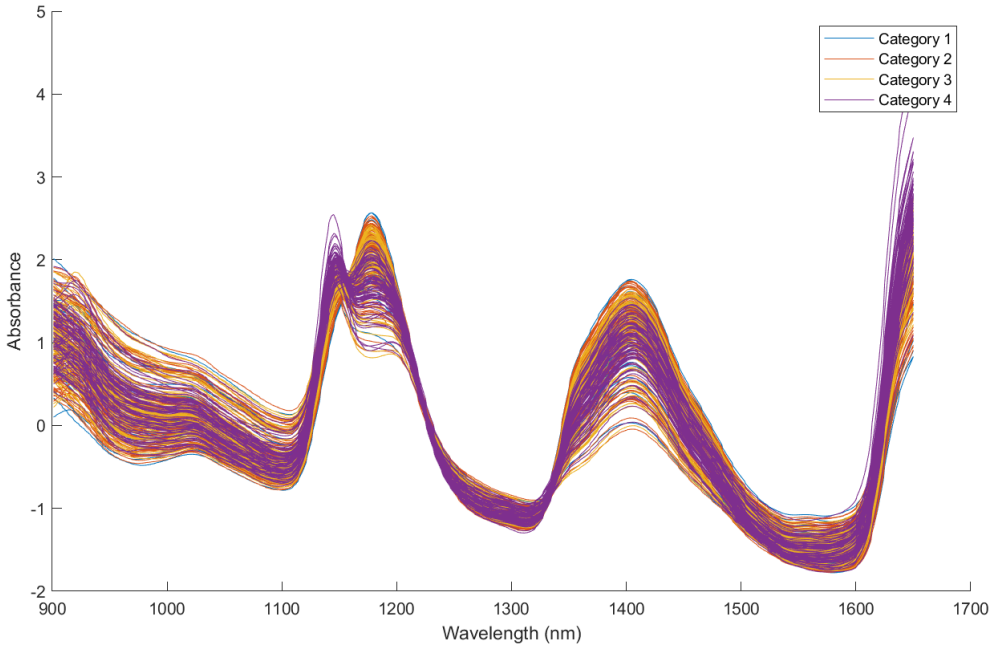


***Figure 11 Smoothed NIR Spectra***

### 5.2.4. Data Cleaning of Smoothed NIR Spectra

Data Cleaning is crucial to ensure the reliability and accuracy of data analysis and improve the robustness of the models developed in the machine learning process. NIR spectra data often contains noise, outliers, and unwanted variations that can negatively impact the predictive performance of models. One popular method for addressing these issues is to employ Partial Least Squares (PLS) regression for outlier detection, which offers a compelling solution due to its ability to handle the inherent complexity and collinearity present in the NIR spectra data. PLS regression excels at capturing latent structures and extracting relevant information from highly correlated variables, making it particularly suitable for NIR spectra data where a high number of variables (wavelengths) relate to observations (TIC) and these variables are often interconnected.

PLS regression outlier detection works by constructing a model that captured the underlying patterns in the smoother NIR spectra and identifying observations that demonstrated significant residuals and deviated significantly from these patterns as outliers (Devarakonda, et al., 2014). With PLS regression outlier detection, 84 spectra were identified as outliers and the remaining 216 spectra were kept for further analysis, as presented in Figure 12.

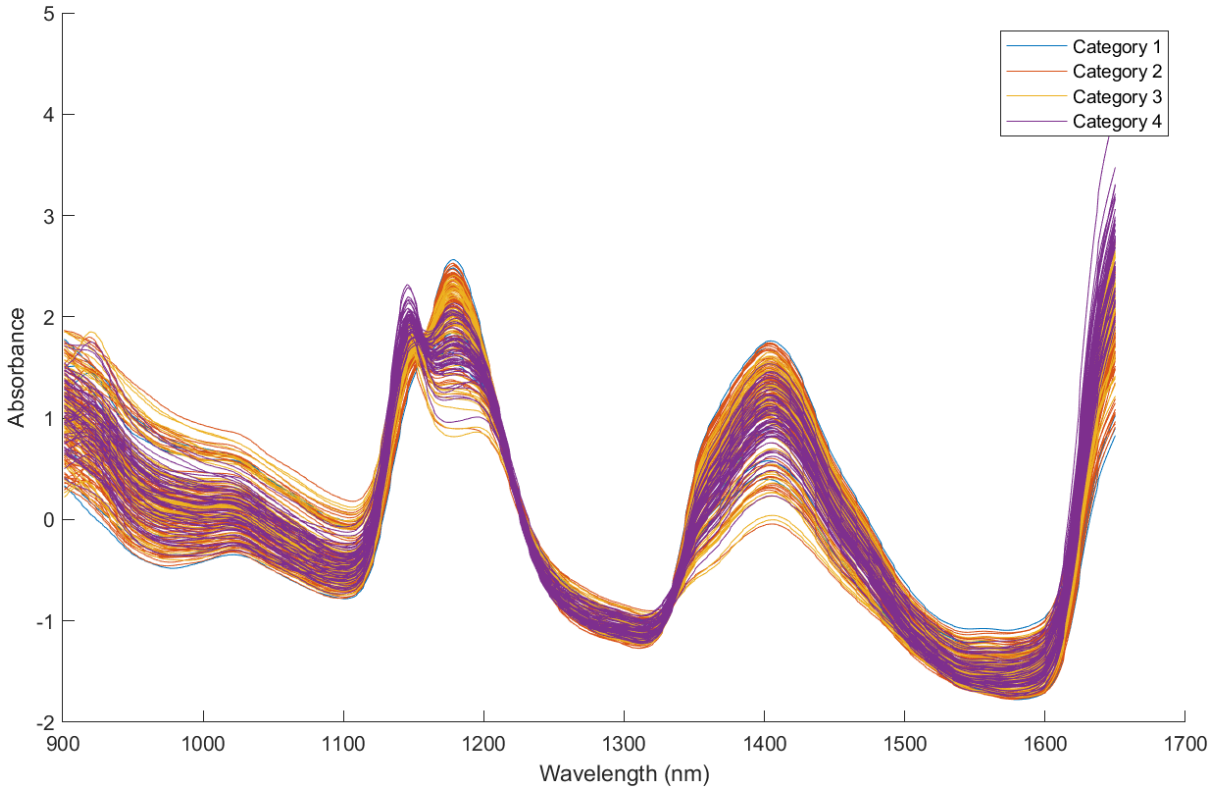


***Figure 12 Cleaned NIR Spectra***

### 5.2.5. Splitting of Cleaned Data

The cleaned NIR spectra and actual TIC values underwent a random partitioning into two distinct subsets: a training dataset, comprising 173 spectra (representing 80 % of the data), and a testing dataset, encompassing 43 spectra (equivalent to 20 % of the data). The training dataset served as the foundation for the construction and refinement of machine learning models through the utilization of MATLAB R2022b. Subsequently, the testing dataset was employed to assess the performance and generalization capabilities of the developed models.

### 5.2.6. Transformation of split data

Data transformation through Principal Component Analysis (PCA) was employed to address issues of multicollinearity and high dimensionality in datasets. PCA is a mathematical technique used for dimensionality reduction and feature extraction in data analysis. Its primary goal is to transform a set of correlated variables, often representing a high-dimensional dataset, into a new set of uncorrelated variables called principal components (PCs). These PCs are ordered by the amount of variance they capture, with the first few PCs retaining the most information present in the original data.

Figure 13 demonstrates the PCA results on the training dataset, revealing that the first 30 PCs effectively account for 99.97 % of the variance present in the original training dataset. These 30 PCs were identified as the transformed variables to be utilized in the subsequent stages of model training. The identical transformation methodology was applied to the testing dataset to assess and validate the final model's performance.

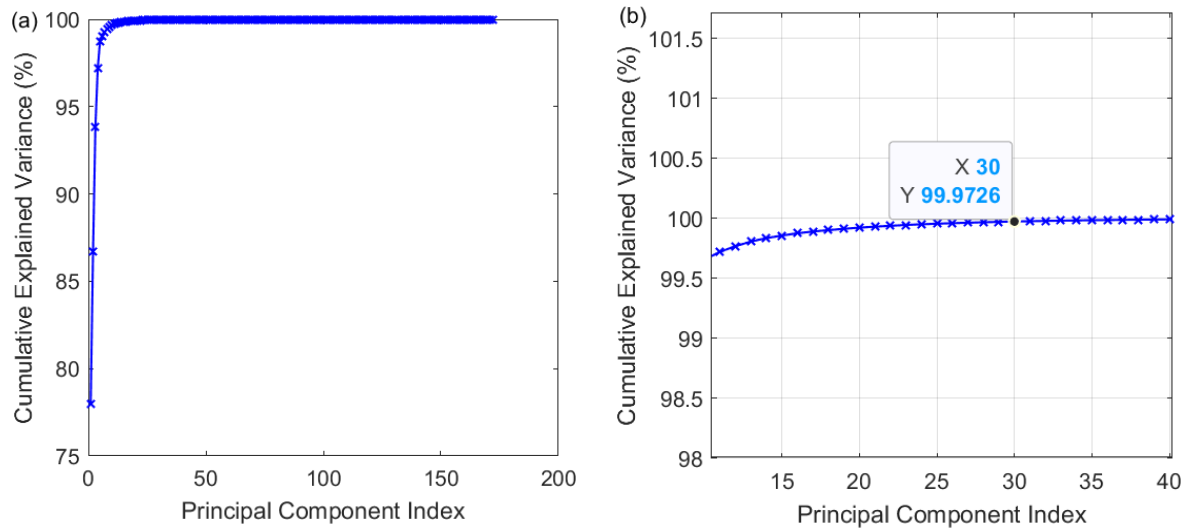


***Figure 13 PCA Results of Training Dataset***

## 5.3. NIR Model Development and Evaluation

Machine learning techniques were employed to evaluate the NIR spectra data after the completion of data pre-processing phase towards the development and evaluation of the models, which included both regression and classification models. These models, integral to the data analysis process, were designed to learn patterns and relationships within the NIR spectra data.

### 5.3.1. NIR Classification Model

An extensive analysis of classification models was undertaken towards construction of predictive models, including Decision Trees, Discriminant Analysis, Naïve Bayes Classifiers, Support Vector Machines (SVM), Nearest Neighbour Classifiers, Kernel Approximation Classifiers, Ensemble Classifiers and Neural Network (NN) Classifiers. It was determined that the Optimizable SVM Classification Model exhibited the most robust performance among the considered models. The selection of the Optimizable SVM Classification Model was made after a comprehensive analysis of its hyperparameters and training outcomes, which are summarized in Table 4.

Figure 14 provides insights into the distribution of both correct and incorrect predictions made by the NIR Optimizable SVM Classification Model on the training dataset. It is evident that Categories 2 and 4 exhibit relatively high true positive rates (TPR) of 75.0 % and 84.4 %, respectively, indicating a good level of effectiveness in the model's classification of these two categories. This suggests that the NIR Optimizable SVM Classification Model successfully identifies and predicts coal/stone dust samples belonging to Categories 2 and 4. Conversely, a notable challenge emerges in the classification of

Category 1, as evidenced by a high false negative rate (FNR) of 83.3 %. The high FNR for Category 1 implies that the model encounters difficulties in accurately identifying coal/stone dust samples belonging to this category. This challenge significantly contributes to the overall accuracy, which is reported at 71.7 %, according to Table 4.

Figure 15 provides a graphical representation of the true positive rate (TPR) versus the false positive rate (FPR) across various classification score thresholds, offering a comprehensive view of the NIR Optimizable SVM Classification Model's performance. The model operating point signifies the specific FPR and TPR values corresponding to the threshold employed by the NIR Optimizable SVM Classification Model for classifying coal/stone dust samples. The area the under curve (AUC) value corresponds to the integral of a ROC curve (TPR values) with respect to FPR from 0 to 1. The AUC value is a measure of the overall quality of the NIR Optimizable SVM Classification Model. The AUC values are in the range 0 to 1, and larger AUC values indicate better classifier performance (Han, et al., 2012). As detailed in Figure 15, AUC values for Categories 2 and 4 exhibit a relatively high-performance level, whereas AUC values for Categories 1 and 3 are comparatively low, indicating a diminished overall performance of the NIR Optimizable SVM Classification Model.

***Table 4 NIR Optimizable SVM Classification Model***

| **Optimized Hyperparameters** | |
|---|---|
| Kernel Scale | 1 |
| Kernel Function | Linear |
| Box Constrain Level | 992.9427 |
| Multiclass Method | One-vs-One |
| Standardize Data | No |
| **Hyperparameter Search Range** | |
| Kernel Scale | 0.001 - 1000 |
| Kernel Function | Gaussian, Linear, Quadratic, Cubic |
| Box Constrain Level | 0.001 - 1000 |
| Multiclass Method | One-vs-One, One-vs-All |
| Standardize Data | True, False |
| **Optimizer: Bayesian Optimization** | |
| Iterations | 30 |
| Training Time Limit | False |
| **Training Result** | |
| Overall Accuracy | 71.7 % |

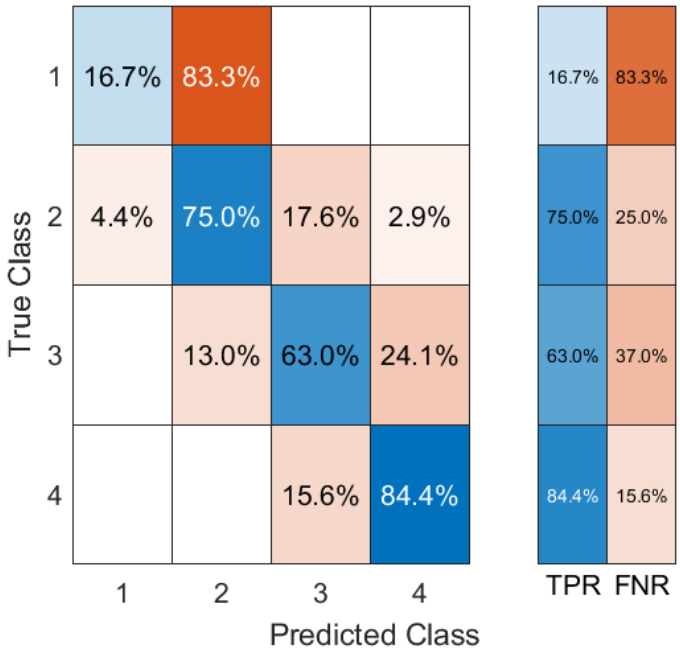


***Figure 14 Confusion Chart for NIR Optimizable SVM Classification Model (Training Dataset)***

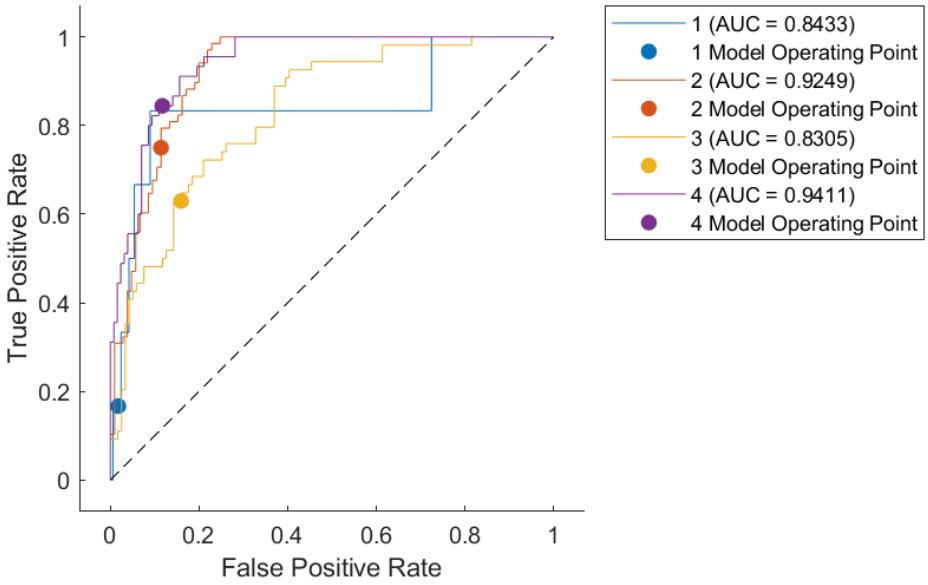


***Figure 15 ROC Curve for NIR Optimizable SVM Classification Model (Training Dataset)***

The NIR Optimizable SVM Classification Model underwent further evaluation process using an independent testing dataset to assess the classifier's predictive performance and its ability to generalize to previously unseen data. As shown in Figure 16, the classifier was employed to predict the categories of 43 coal/stone dust samples within the testing dataset, resulting in an overall accuracy rate of 58.1 %. It's worth noting that this accuracy value deviates from the performance observed during the training phase with the training dataset. This discrepancy can be attributed to the specific challenges encountered by the NIR Optimizable SVM Classification Model, particularly in accurately classifying Category 1 samples. In comparison, the classification model demonstrated a high accuracy of 90.0 % for Category 4.

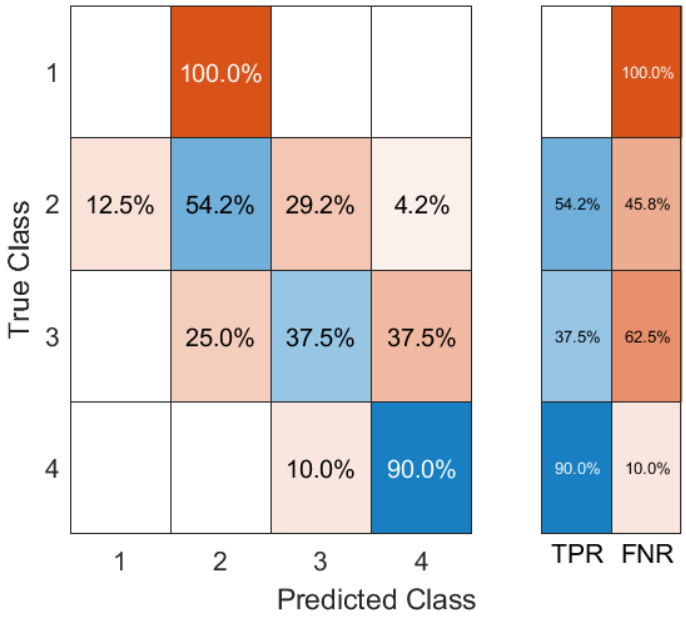


***Figure 16 Confusion Chart for NIR Optimizable SVM Classification Model (Testing Dataset)***

### 5.3.2. NIR Regression Model

A comprehensive assessment of various regression models was conducted, including Linear Regression Models (LRM), Regression Trees, Support Vector Machines (SVM), Gaussian Process Regression (GPR) Models, Kernel Approximation Regression Models, Ensemble of Trees and Neural Networks (NN) with the objective of finding the most suitable regression model for the pre-processed NIR spectra.

It was determined that the LRM outperformed the other models and emerged as the optimal choice. The selection of LRM was based on a meticulous analysis of its hyperparameters and training outcomes. Table 5 summarizes the coefficients and performance metrics for this regression model, revealing a Root Mean Squared Error (RMSE) of 2.87 % and $R^2$ of 0.81.

***Table 5 NIR Linear Regression Model***

| **Coefficients** | | | | | | | |
|---|---|---|---|---|---|---|---|
| Intercept | 80.8191 | PC 8 | -0.2928 | PC 16 | -3.7946 | PC 24 | -3.5368 |
| PC 1 | -0.0190 | PC 9 | -0.8567 | PC 17 | -0.2594 | PC 25 | -1.4874 |
| PC 2 | 0.8490 | PC 10 | 0.5822 | PC 18 | -1.8702 | PC 26 | 0.2694 |
| PC 3 | -0.0532 | PC 11 | -2.1151 | PC 19 | -0.3007 | PC 27 | 1.6843 |
| PC 4 | 0.5067 | PC 12 | -1.0042 | PC 20 | -2.1594 | PC 28 | -0.4941 |
| PC 5 | -0.0630 | PC 13 | 0.1581 | PC 21 | 0.5239 | PC 29 | -6.2874 |
| PC 6 | -0.7131 | PC 14 | -2.6843 | PC 22 | -2.8802 | PC 30 | -8.0536 |
| PC 7 | -0.4722 | PC 15 | -0.8340 | PC 23 | 3.2498 | | |
| **Training Results** | | | | | | | |
| RMSE | | 2.87 % | | $R^2$ | | 0.81 | |

Figure 17 visually presents the performance of the NIR LRM. As shown in Figure 17(a), the diagonal line represents a perfect prediction scenario where actual values equal predicted one. Points along this line indicate accurate predictions. The tight cluster of points around the diagonal line suggests that the model makes accurate predictions for a majority of the data. As illustrated in Figure 17(b), residuals fluctuate randomly near the zero line, suggesting that the model captures the underlying patterns in the training dataset well.

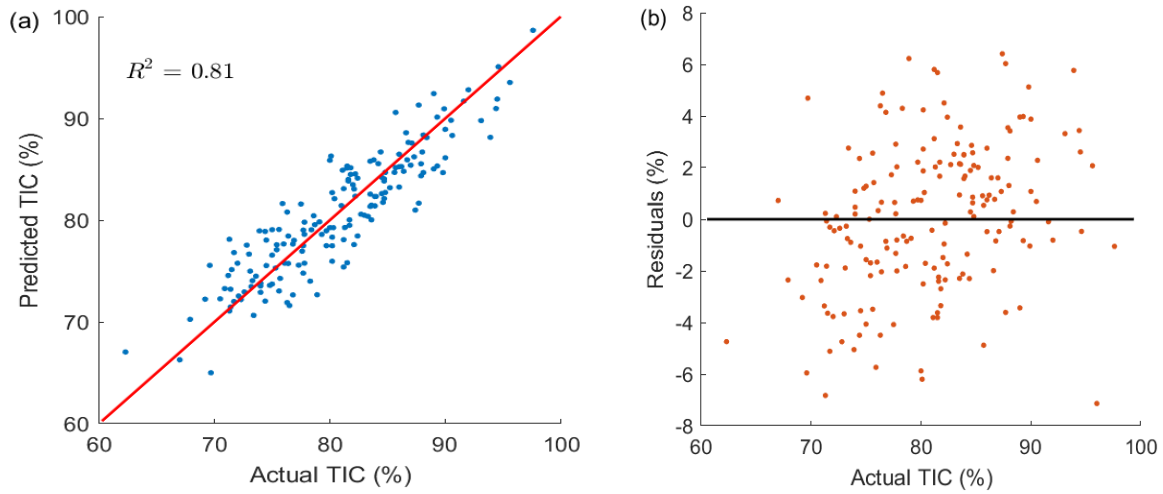


***Figure 17 (a) Comparison of Actual and Predicted TIC for NIR LRM (Training Dataset); (b) Residuals for NIR LRM (Training Dataset)***

The NIR LRM underwent a comprehensive evaluation using an independent testing dataset to assess the model's predictive capabilities and its generalization to unseen data. As illustrated in Figure 18, the NIR Linear regression model successfully predicted the TIC values for a set of 43 coal/stone dust samples within the testing set. The evaluation yielded notable performance metrics with R-squared ($R^2$) value of 0.82 and a Root Mean Square Error (RMSE) of 2.67 %. These results closely aligned with the performance metrics obtained during the training phase using the training dataset. Such close correspondence between training and testing results indicates that the model achieved a balance between accuracy and generalization, suggesting that it did not suffer from overfitting and demonstrated stability in its predictive performance. This outcome underscores the robustness and reliability of the NIR LRM in capturing the underlying patterns in the data.

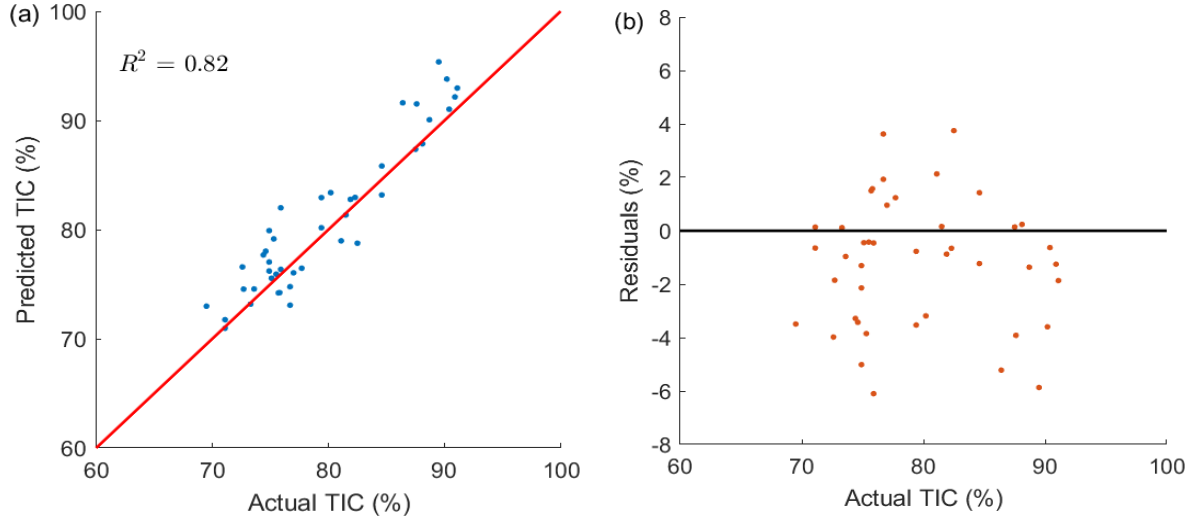


***Figure 18 (a) Comparison of Actual and Predicted TIC for NIR LRM (Testing Dataset); (b) Residuals for NIR LRM (Testing Dataset)***

### 5.3.3. NIR Classification and Regression Model Comparison

Two distinct NIR models were successfully developed based on the machine learning technique: regression and classification.

The NIR Optimizable SVM Classification Model demonstrated high accuracy, reaching 84.4 % for Category 4. Nevertheless, the overall accuracy of the model stood at 71.7 %, which fell slightly short of the project objectives outlined in Section 2.4. This shortfall was primarily attributed to challenges encountered by the model in accurately categorizing instances within Category 1.

The NIR LRM, on the other hand, yielded promising results, achieving a RMSE of 2.87 % and $R^2$ of 0.81, aligning well with the objectives outlined in Section 2.4.

# 6.0 Model Development for Lightnovo miniRaman Portable Spectrometer

## 6.1. Raman Spectra Data Acquisition

The initiation of Raman spectra data acquisition involved the systematic sample scanning utilizing the Lightnovo miniRaman portable spectrometer. A total of 400 samples underwent scanning, comprising 100 coal samples and 300 coal/stone dust samples.

The Miraspec software, provided by Lightnovo, facilitated the configuration of the parameters of the Lightnovo miniRaman portable spectrometer and recording Raman spectra data throughout the scanning process. The scanning parameters were defined as follows: a laser power of 10 mW, an exposure time of 250 ms, and a repetition of 25 scans. Each spectrum's intensity data was saved individually, and each file was assigned a unique identifier corresponding to its respective scan.

The Raman sample scanning process incorporated the following techniques:

### 6.1.1. Calibration of Lightnovo miniRaman Portable Spectrometer

Prior to commencing sample scanning, Lightnovo miniRaman portable spectrometer underwent calibration following the Standard Operation Procedure provided by the supplier. The calibration process involved the utilization of a polystyrene standard sample to ensure the precision in wavenumber and intensity measurements.

### 6.1.2. Background Correction

Raman analysis is susceptible to various interferences, such as, ambient light sources and signals from the sample containers, which can contribute to the background signal. Therefore, background correction was implemented during sample scans to subtract unwanted background and sample container signals, enhancing the accuracy and reliability of the recorded Raman spectra data.

### 6.1.3. Baseline Correction

Fluorescence poses a common challenge in Raman spectroscopy, especially for low-maturity samples. Additionally, the broad bands in the Raman spectra of carbonaceous solid fuels, like coal, can easily be confused with the fluorescence background (Quirico, et al., 2005), leading to a significant baseline shift. Therefore, baseline correction was applied during sample scans using Rolling Circle filter with a radius of 750 and a scale Y of 0.01.

### 6.1.4. Smoothing

Although the optimized Raman scanning parameters typically yield a high signal-to-noise ratio (SNR) in Raman spectra, the nature of coal and coal/stone dust samples, combined with the sensitivity to thermal effects and the low laser power and frequency of the Lightnovo miniRaman portable spectrometer in this project, resulted in Raman spectra data with notable noise disturbances. Therefore, smoothing was applied during sample scans to remove noise from the Raman spectra data using Savitzky-Golay filter with a radius of 25 and the order of 6, enabling the extraction of Raman signals with less ambiguity.

The scanned samples were categorized into five distinct groups, as outlined in Table 3. The raw Raman spectra of 300 coal/stone dust samples are presented in Figure 19.

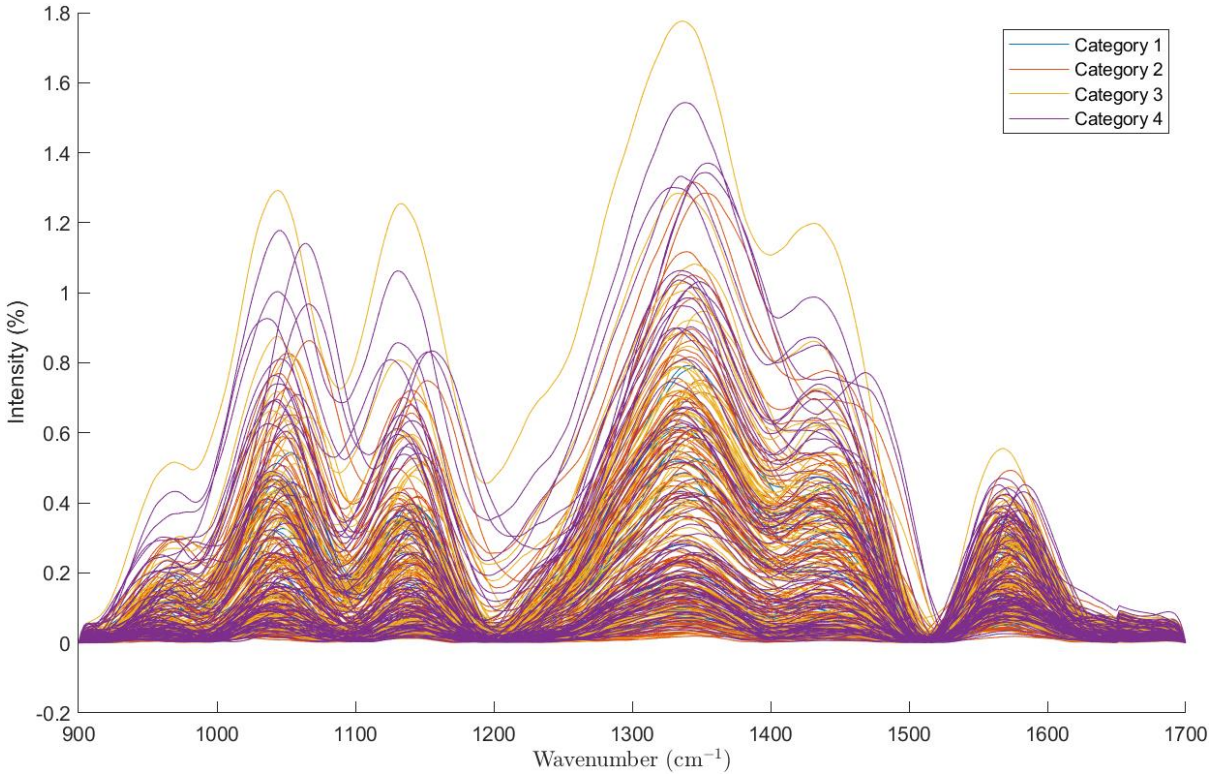


***Figure 19 Raw Raman Spectra***

## 6.2. Raman Spectra Data Pre-Processing

The raw Raman spectra of 300 coal/stone dust samples underwent data pre-processing and cleaning, utilizing a combination of MATLAB and Python. This step was crucial in preparing the Raman spectra data for the subsequent machine learning processes.

The pre-processing and cleaning involved the following steps to enhance the quality and reliability of the Raman spectra data:

### 6.2.1. Alignment of Raw Raman Spectra

Raman spectra alignment is a crucial step in the data pre-processing and analysis pipeline to ensure the consistency and comparability of the acquired raw Raman spectra. The primary goal is to correct for potential shifts along the wavenumber axis, which may arise from instrumental or environmental variations in the starting and ending wavenumbers during data acquisition. A common approach involves utilizing cross-correlation to determine the optimal alignment between a selected reference spectrum and the remaining spectra in the Raman spectra data. The alignment was achieved through interpolation, ensuring that corresponding wavenumbers across spectra were precisely matched (Chen, et al., 2018). Figure 20 presents the aligned Raman spectra.

### 6.2.2. Normalization of Aligned Raman Spectra

Normalization is essential when predicting the concentration of similar style samples, like different coal samples dosed with the same stone dust, using Raman spectra. Variations in coal samples can introduce inherent differences in Raman intensity due to factors such as mineral composition. Normalization is crucial to eliminate these intensity variations, ensuring that concentration predictions are based on the intrinsic molecular features rather than sample-specific intensity differences. It ensures that predictive models focus on the relevant concentration-related information, making them more resilient to experimental variations and improving their generalizability across diverse sample sets.

The choice of normalization method depends on the nature of the dataset, and selecting an appropriate method enhances the performance and interpretability of subsequent machine learning models. Due to the inherent variations in Raman intensity arising from different mineral compositions in coal samples,

an extensive normalization analysis was conducted. This analysis encompassed various normalization techniques, including min-max normalization (Han, et al., 2012), area normalization (Chirala & Kumar , 1990), vector normalization, z-score normalization (Han, et al., 2012), logarithmic normalization, and custom scaling (Han, et al., 2012). Custom scaling was implemented through a multiplication factor applied to the aligned Raman spectra, ensuring uniform intensity values at 942 $cm^{-1}$ for all sample scans. Following a comprehensive evaluation, it was determined that custom scaling yielded the most effective normalization results. The outcome of this investigation is presented in Figure 21.

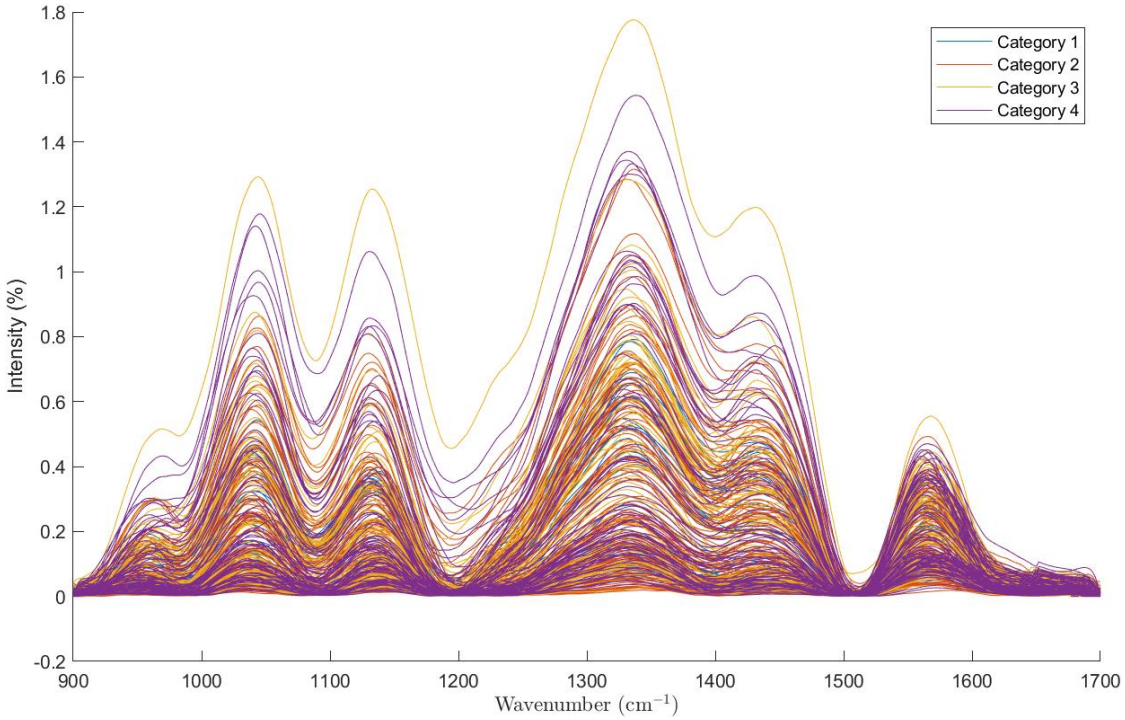


***Figure 20 Aligned Raman Spectra***

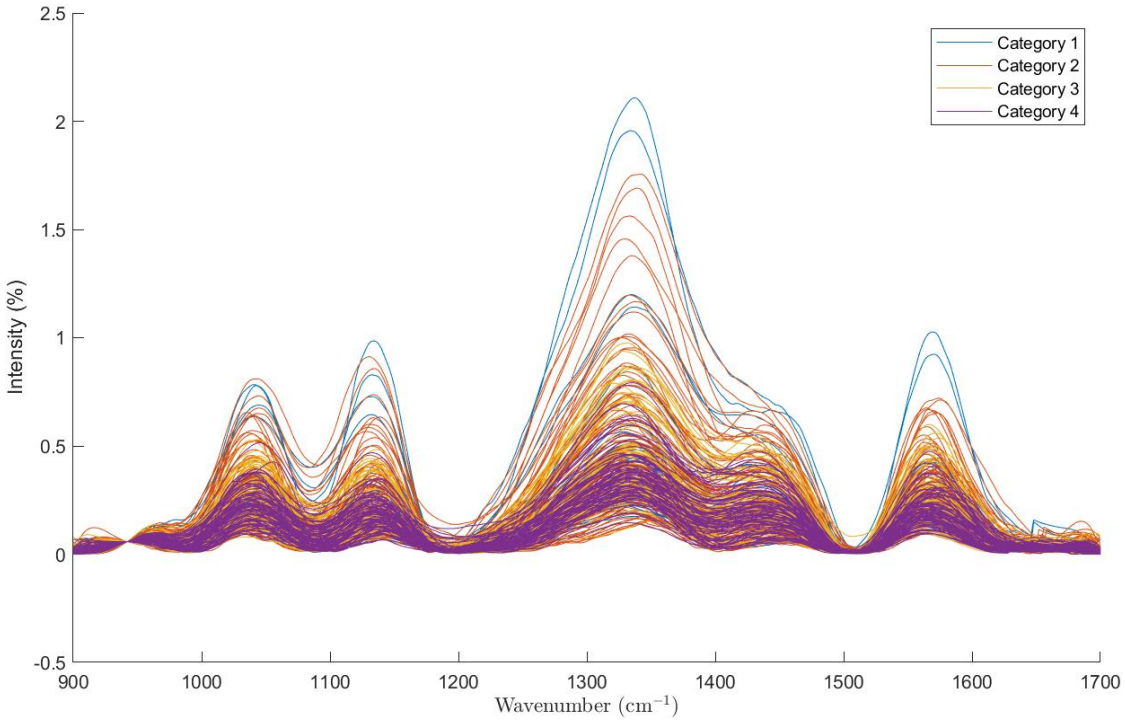


***Figure 21 Normalized Raman Spectra***

### 6.2.3. Data Cleaning of Normalized Raman Spectra

Tukey's fence outlier detection technique (Schwertman, et al., 2004) was applied to remove outliers to improve the quality and reliability of the normalized Raman spectra. By excluding extreme values beyond the established fences, this method aimed to improve the robustness of the Raman spectra data. Notably, variations in Raman intensity were observed to be associated with fluctuations in TIC values. As shown in Figure 22, the data cleaning procedure was implemented on a per-category basis, allowing for the removal of extreme values within each specific category. This approach ensured that outliers, which might have aligned with neighbouring categories but did not reflect extreme values across the entire dataset, were appropriately addressed. Figure 23 presents the cleaned Raman spectra, while Table 6 summarizes the data cleaning, 71 spectra identified as outliers and 229 spectra retained for subsequent analysis.

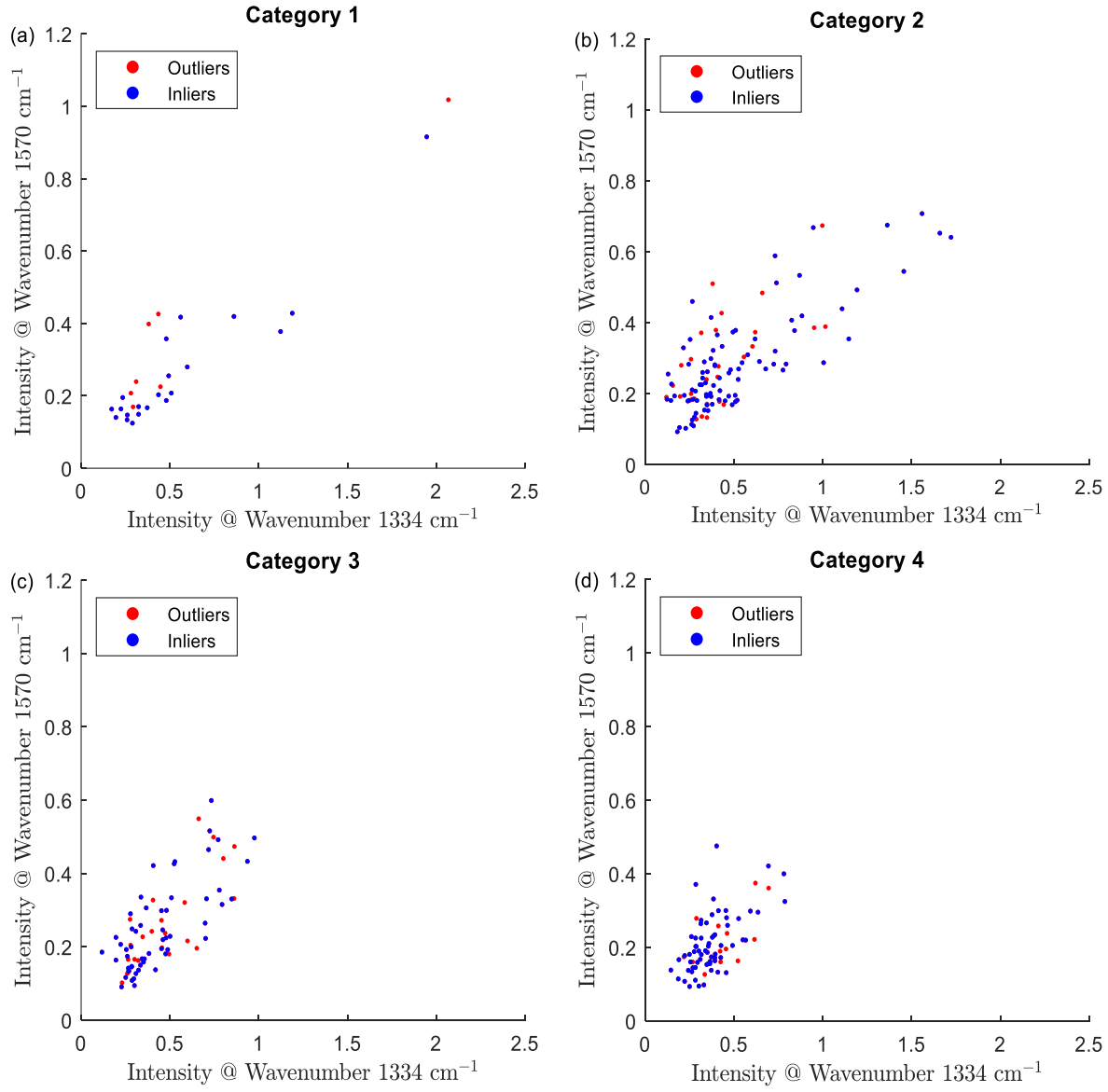


***Figure 22 Tukey's Fence Data Cleaning per Category***

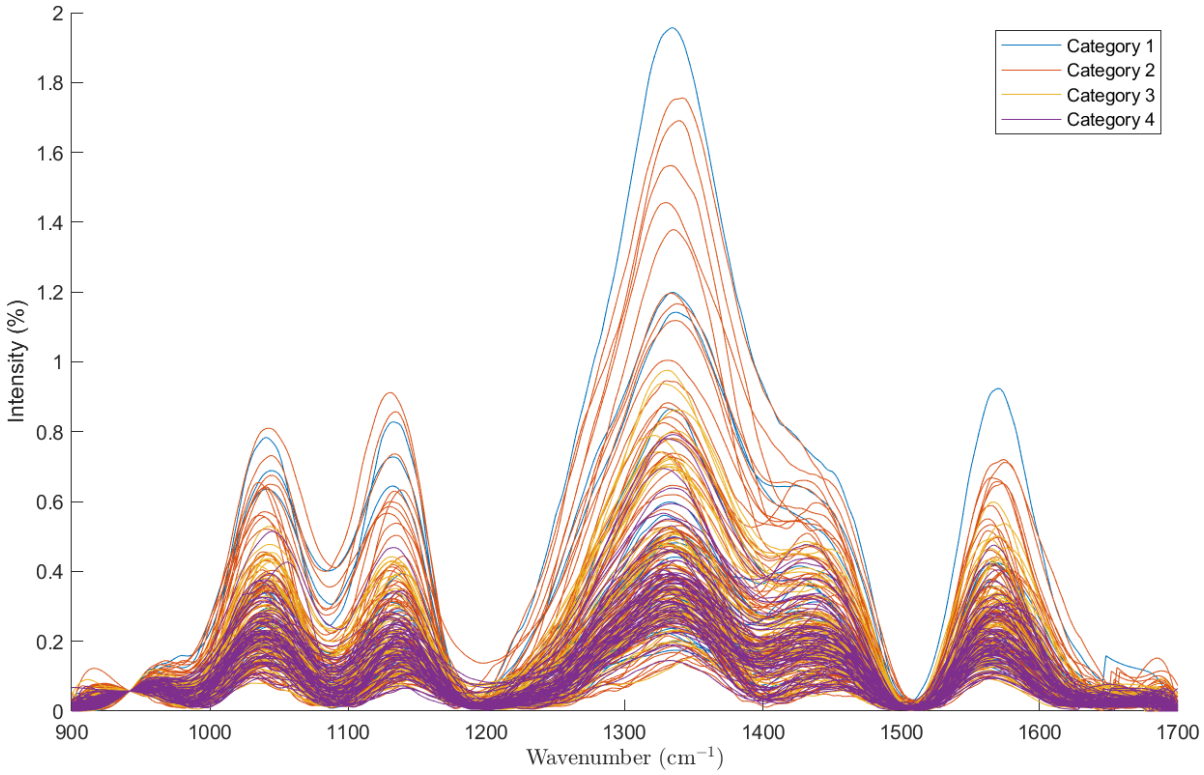


***Figure 23 Cleaned Raman Spectra***

***Table 6 Summary of Tukey's Fence Data Cleaning***

| | Inliers | Outliers | Total |
|---|---|---|---|
| **Category 1** | 21 | 7 | 28 |
| **Category 2** | 88 | 28 | 116 |
| **Category 3** | 56 | 22 | 78 |
| **Category 4** | 64 | 14 | 78 |
| **Total** | 229 | 71 | 300 |

#### 6.2.4. Splitting of Cleaned Data

The cleaned Raman spectra and actual TIC values underwent a systematic random partitioning, resulting in the creation of two distinctive subsets: a training dataset comprising 184 spectra, representing 80 % of the dataset, and a testing dataset consisting of 45 spectra, equivalent to 20 % of the data. The training dataset played a fundamental role in the formulation and refinement of machine learning models, leveraging the capabilities of MATLAB R2022b. Following model development, the testing dataset was employed to assess the performance and generalization aptitude of the derived models.

## 6.3. Raman Model Development and Evaluation

Machine learning methodologies were applied after the completion of data pre-processing to develop and evaluate Raman regression and classification models. These models were engineered to discern patterns and relationships embedded within the dataset.

### 6.3.1. Raman Classification Model

A comprehensive examination of classification models was conducted utilizing the training dataset to construct predictive models, encompassing a range of methodologies, including Decision Trees, Discriminant Analysis, Naïve Bayes Classifiers, Support Vector Machines (SVM), Nearest Neighbour Classifiers, Kernel Approximation Classifiers, Ensemble Classifiers and Neural Network (NN) Classifiers. After the analysis, it was concluded that the Optimizable Tree demonstrated the most robust performance among the models under consideration. The decision to select the Optimizable Tree was based on the evaluation of its hyperparameters and training outcomes, as detailed in **Table 7**. This selection process ensures the adoption of a model that exhibits optimal performance and reliability for this classification task.

***Table 7 Raman Optimizable Tree Classification Model***

| **Optimized Hyperparameters** | |
|---|---|
| Surrogate Decision Splits | Off |
| Maximum Number of Splits | 14 |
| Split Criterion | Twoing Rule |
| **Hyperparameter Search Range** | |
| Maximum Number of Splits | 1 - 183 |
| Split Criterion | Gini's Diversity Index<br>Twoing Rule<br>Maximum Deviation Reduction |
| **Optimizer: Bayesian Optimization** | |
| Iterations | 30 |
| Training Time Limit | False |
| **Training Result** | |
| Overall Accuracy | 39.1 % |

Figure 24(a) illustrates the Raman intensities at wavenumbers 1334 and 1570 $cm^{-1}$ grouped by the respective categories. A notable observation is the absence of distinct separation among the categories, suggesting inherent complexities that pose challenges for the Raman Optimizable Tree classification model in accurately classifying coal/stone dust samples based on their Raman spectra. Moreover, in Figure 24(b), a presence of misclassifications is evident, underscoring the suboptimal performance of the Raman Optimizable Tree classification. This further underscores the difficulty the model faces in effectively distinguishing coal/stone dust samples.

Figure 25 provides insights into the distribution of both correct and incorrect predictions made by the Raman Optimizable Tree classification model on the training dataset. It is evident that Categories 2 and 4 exhibit relatively high true positive rates (TPR) of 49.3 % and 46.0 %, respectively, indicating a good level of effectiveness in the model's classification of these two categories. This suggests that the Raman Optimizable Tree classification model successfully identifies and predicts coal/stone dust samples belonging to Categories 2 and 4. Conversely, a notable challenge emerges in the classification of Category 1, as evidenced by a high false negative rate (FNR) of 94.7 %. The high FNR for Category 1 implies that the model encounters difficulties in accurately identifying coal/stone dust samples belonging

to this category. This challenge significantly contributes to the overall accuracy, which is reported at 39.1 %, according to Table 7.

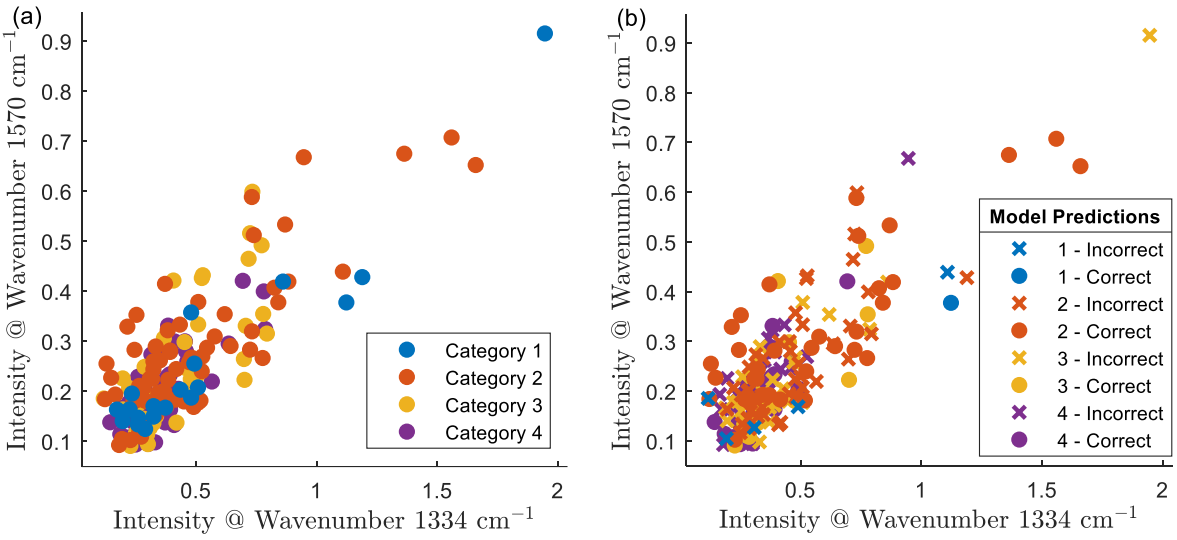


***Figure 24 (a) Raman Intensities at Wavenumber 1334 and 1570 cm-1 of Cleaned Spectral per Category; (b) Optimizable Tree Model Predications (Training Dataset)***

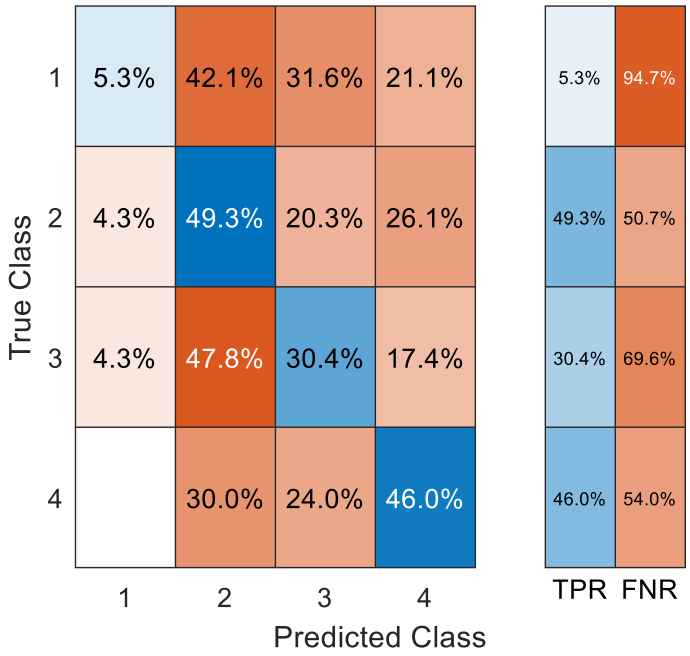


***Figure 25 Confusion Chart for Raman Optimizable Tree Classification Model (Training Dataset)***

Figure 26 provides a graphical representation of the true positive rate (TPR) versus the false positive rate (FPR) across various classification score thresholds, offering a comprehensive view of the Raman Optimizable Tree classification model's performance. The model operating point signifies the specific FPR and TPR values corresponding to the threshold employed by the Raman Optimizable Tree classification model for classifying coal/stone dust samples. The area the under curve (AUC) value corresponds to the integral of a ROC curve (TPR values) with respect to FPR from 0 to 1. The AUC value is a measure of the overall quality of the Optimizable Tree. The AUC values are in the range 0 to 1, and larger AUC values indicate better classifier performance (Han, et al., 2012). As detailed in Figure

26, AUC values for Categories 2 and 4 exhibit a relatively high-performance level, whereas AUC values for Categories 1 and 3 are comparatively low, indicating a diminished overall performance of the Raman Optimizable Tree classification model.

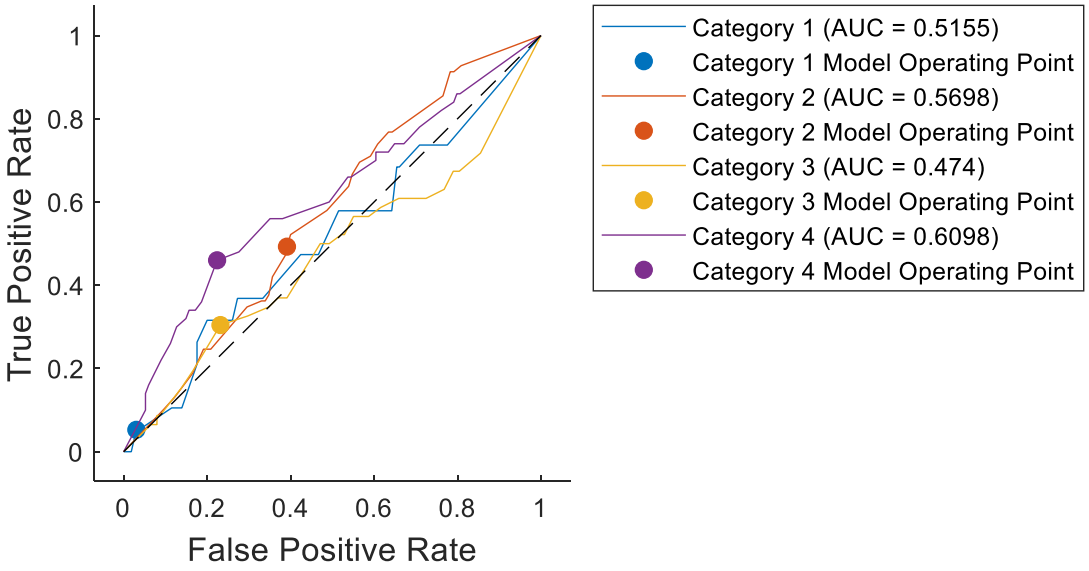


***Figure 26 ROC Curve for Raman Optimizable Tree Classification Model (Training Dataset)***

The Raman Optimizable Tree classification model underwent a comprehensive evaluation process using the testing dataset to assess its predictive performance and generalization capabilities to previously unseen data. As shown in Figure 27, the model was applied to predict the categories of 45 coal/stone dust samples within the testing dataset, yielding an overall accuracy rate of 37.8 %. Notably, this accuracy aligns closely with the performance observed during the training phase with the training dataset, indicative of the sufficiency of the training dataset for model training and the absence of overfitting or underfitting. Furthermore, this classification model exhibited a notable accuracy of 68.4 % for Category 2. In contrast, the accuracies for Categories 1 and 3 were considerably lower, with 0 % and 10.0 %, respectively.

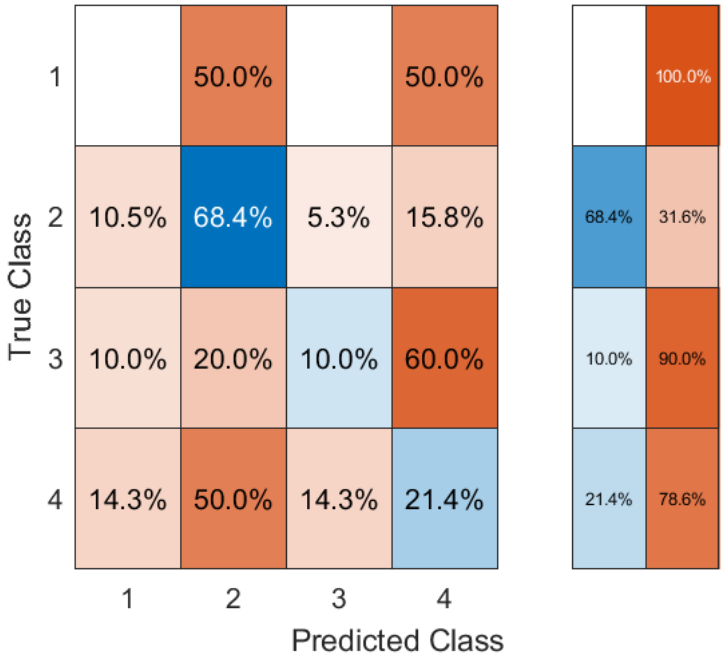


***Figure 27 Confusion Chart for Raman Optimizable Tree Classification Model (Testing Dataset)***

### 6.3.2. Raman Regression Model

A thorough evaluation of multiple regression models, encompassing Linear Regression Models, Regression Trees, Support Vector Machines (SVM), Gaussian Process Regression (GPR) Models, Kernel Approximation Regression Models, Ensemble of Trees and Neural Networks (NN), was undertaken with the aim of identifying the most suitable regression model for the pre-processed Raman spectra data. Subsequent analysis revealed that the Optimizable Regression Tree surpassed the performance of the other models, emerging as the optimal choice. The selection of the Optimizable Regression Tree was informed by the examination of its hyperparameters and training outcomes, as summarized in Table 8.

***Table 8 Raman Optimizable Regression Tree Model***

| **Optimized Hyperparameters** | |
|---|---|
| Surrogate Decision Splits | Off |
| Minimum Leaf Size | 69 |
| **Hyperparameter Search Range** | |
| Minimum Leaf Size | 1 -92 |
| **Optimizer: Bayesian Optimization** | |
| Iterations | 30 |
| Training Time Limit | False |
| **Training Result** | |
| RMSE | 7.324 % |
| $R^2$ | 0.04 |

The training outcomes are graphically depicted in Figure 28. The scatter plot reveals a notable deviation of data points from the diagonal line, suggesting suboptimal predictive performance utilizing the Raman Optimizable Regression Tree model.

The Raman Optimizable Regression Tree model underwent a thorough evaluation utilizing the testing dataset to assess its predictive capabilities and generalization to previously unseen data. As depicted in Figure 29, the model exhibited limited success in predicting the TIC values for a set of 45 coal/stone dust samples within the testing dataset, yielding an R-squared ($R^2$) value of 0.01 and a Root Mean Square Error (RMSE) of 7.3236 %. These outcomes closely mirrored the performance metrics acquired during the training phase with the training dataset. The convergence of training and testing results suggests that the model achieved a balance between accuracy and generalization, indicative of its resilience against overfitting and its consistent predictive stability.

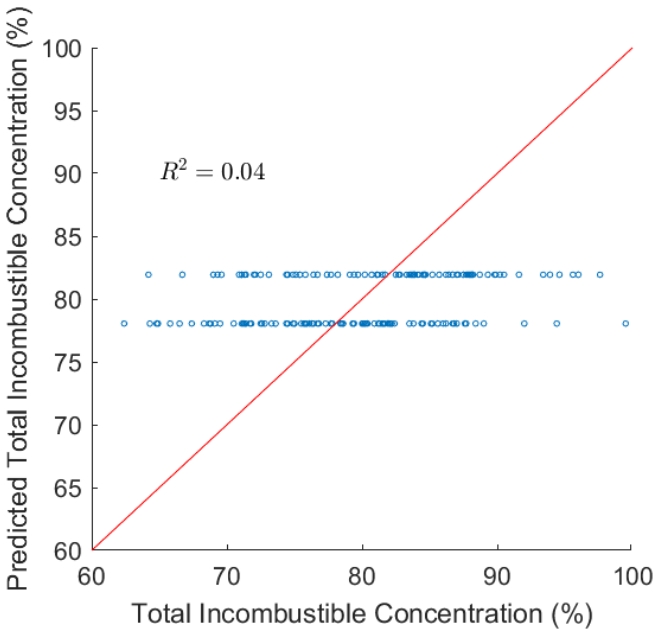


***Figure 28 Comparison of Predicted and Actual TIC for Raman Optimizable Regression Tree Model (Training Dataset)***

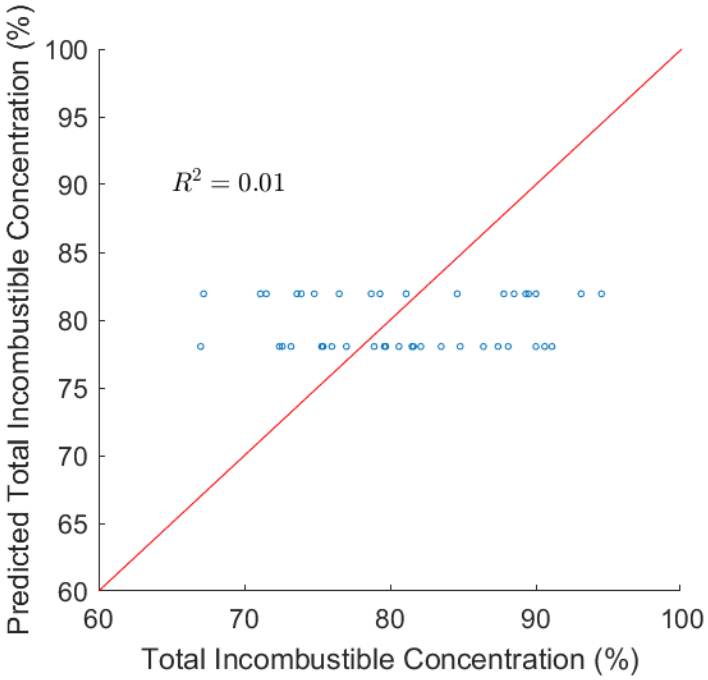


***Figure 29 Comparison of Predicted and Actual TIC for Raman Optimizable Regression Tree Model (Testing Dataset)***

### 6.3.3. Raman Classification and Regression Model Comparison

Two distinct models, one for classification and another for regression, were developed for the Lightnovo miniRaman portable spectrometer using machine learning techniques.

The Raman Optimizable Tree classification model exhibited notable success, achieving an accuracy of 68.4 % specifically for Category 2. However, the overall accuracy of the classification model reached 37.8 %, which did not meet the predefined project objective outlined in Section 2.4.

On the other hand, the Raman Optimizable Regression Tree model did not yield favourable results, as evidenced by an R-squared ($R^2$) value of 0.01 and a Root Mean Square Error (RMSE) of 7.3236 %. These outcomes fell short of the initial project objectives specified in Section 2.4.

# 7.0 NIR and Raman Model Comparison

The NIR Linear Regression Model (LRM) exhibited superior predictive performance, achieving an RMSE of 2.87 % and an $R^2$ of 0.81, as highlighted in Section 5.3.3, in contrast to the NIR Optimizable SVM Classification Model. These results align closely with the objectives outlined in Section 2.4.

The Raman Optimizable Tree Classification Model demonstrated improved prediction performance with an overall accuracy of 37.8 %, when compared to the Raman Optimizable Regression Tree model, as discussed in Section 6.3.3. However, it fell short of meeting the predefined project objective specified in Section 2.4.

Overall, the application of the Stellarnet NIR ADK portable spectrometer yielded the most favourable predictive performance in rapid TIC analysis, notably through the development of the NIR LRM. On the other hand, the Lightnovo miniRaman portable spectrometer did not deliver optimal predictive performance in real-time stone dust analysis, whether through regression or classification models.

The less favourable predictive outcome for the Lightnovo miniRaman portable spectrometer can be attributed to several variables. One of the variables is the moisture content in samples: as the water can have an intensive absorption of the NIR light and reduce its Raman scattering light signal (Xu, et al., 2021), the moisture content in coal and coal/stone dust samples might have impacted the accuracy of their Raman spectra.

Additionally, the fundamental principles of Raman spectroscopy contribute to less favourable predictive outcome for the Lightnovo miniRaman portable spectrometer. The intensity of Raman scattering can be defined according to Equation (1):

$$I = K \times l \times \delta^2 \times w^4, \qquad \textbf{(1)}$$

where: $K$ is a constant, $\delta$ is the polarizability of electrons in a molecule, $l$ and $w$ are the power and frequency of the laser. $K$ depends on various factors, including the nature of the sample, the efficiency of the Raman instrument and the units used for power, polarizability and frequency. The intensity of Raman scattering, $I$, is highly dependent on the frequency of the laser, and the $w^4$ term in the equation indicates a strong dependence on this factor (Smith & Dent, 2005).

Furthermore, the Raman signal induced by the near-infrared (NIR) (785nm) laser is weak according to Equation (1), despite the low power of NIR laser being the main advantage of Lightnovo miniRaman portable spectrometer, which is typically challenging to induce the fluorescence in most materials (Czamara, et al., 2015). Consequently, Raman scanning often necessitates a higher laser power, typically from 100 mW to 500 mW (Xu, et al., 2021), instead of the low laser power of up to 50 mW Lightnovo miniRaman portable spectrometer. This elevated laser power requirement poses a risk of thermal damage to the sample, especially for dark samples, such as, coal and coal/stone dust samples.

To address the various issue, dispersing coal and coal/stone dust samples in dilutants, such as, KCl and KBr is preferred during Raman analysis. These substances serve as effective thermal conductors, mitigating the potential thermal damage caused by the higher laser power during Raman scanning (Smith & Dent, 2005).

# 8.0 Conclusions

The project has successfully achieved the objectives outlined in Section 2.4, which included the selection of two commercially available spectrometers for evaluation, the preparation of 300 coal/stone dust samples, the development of both classification and regression models for the chosen spectrometers, and the comprehensive comparison of the performance of the selected spectrometers.

The NIR Linear Regression Model (LRM) exhibited superior predictive performance, achieving an RMSE of 2.87 % and an $R^2$ of 0.81, as highlighted in Section 5.3.3. These results align closely with the objectives outlined in Section 2.4 of the project.

On the other hand, the Raman Optimizable Tree Classification Model demonstrated an overall accuracy of 37.8 %, as discussed in Section 6.3.3. However, it fell short of meeting the predefined project objective specified in Section 2.4.

In conclusion, the application of the Stellarnet NIR ADK portable spectrometer yielded the most favourable predictive performance in rapid TIC analysis, notably through the development of the NIR LRM. Conversely, while the Lightnovo miniRaman portable spectrometer did not deliver optimal predictive performance in real-time stone dust analysis, whether through regression or classification models, it must be noted that the analysis of data for the Raman spectrometer was not as comprehensive as for the Stellarnet NIR ADK spectrometer due to time constraints.

# 9.0 Recommendations and Future Developments

Based on the results obtained to-date, certain areas have been identified for project improvement, encompassing sample selection, data pre-processing, and analysis.

## 9.1. Sample Selection

Given that the chosen coal samples encompassed a variety of both fresh and aged samples spanning a 20-year timeframe, the oxidation process in aged coal samples could potentially influence spectrum readings. Hence, incorporating fresh coal samples from coal mines into the study could facilitate an examination of the impact of coal sample aging. This exploration aims to ascertain whether the selection of fresh coal samples contributes to enhancing model development.

## 9.2. Data Pre-Processing and Analysis

Further data pre-processing and analysis should be undertaken to improve results for both spectrometers as follows:

### 9.2.1. Stellarnet NIR ADK Portable Spectrometer

The NIR Optimizable SVM Classification Model demonstrated an overall good prediction capability but fell short in recognizing Category 1 data. This is a common problem in implementing machine learning algorithm with imbalanced data, which was the case with Category 1 samples, which were under-represented. Therefore, in further research, the use of appropriate data balancing techniques, for example, SMOTE techniques (Liu, et al., 2023) to increase Category 1 size would be explored.

### 9.2.2. Lightnovo miniRaman Portable Spectrometer

The results indicated that the Lightnovo miniRaman portable spectrometer did not deliver optimal predictive performance in real-time stone dust analysis, whether through regression or classification models. However, this inadequate performance could be attributed to many factors ranging from data acquisition to the model training. In addition, due to the late arrival of the Lightnovo miniRaman portable spectrometer, as compared to the Stellarnet NIR ADK portable spectrometer, thorough performance analysis was not possible in the timeframe allocated for the completion of the project. Therefore, the

following steps will be undertaken in the near future toward more thorough evaluation of the Lightnovo miniRaman portable spectrometer:

1. Data acquisition: additional Raman spectra will be acquired with the laser power set to <0.40 mW, as suggested by recent study related to coal samples undertaken (Vergara Sassarini, et al., 2023) with further literature review of the state-of-the-art.
2. Data pre-processing: a more systematic deconvolution process of the Raman spectra data will be applied to assess the Raman parameters (e.g., peak position, width, area and intensity) for individual bands (Ba, et al., 2022).
3. Model development: other algorithms with successful application for spectral data will be explored (Qin, et al., 2024).
4. Additional time will be allocated for data analysis for the Raman spectrometers because studies related to coal for the Raman parameters are very limited.

# 10.0 Acknowledgement

The author would like to express gratitude to the Coal Service Health and Safety Trust for their generous funding under the Project No. 20663 entitled “System Demonstrator of a Portable NIR Spectrometer for Rapid Stone Dust Compliance Testing”, which greatly contributed to the success of this project.

Special thanks to Professor Amoussou Coffi Adoko from the School of Mining and Geosciences, Nazarbayev University, for his invaluable contribution to data processing and machine learning analysis, enhancing the project's overall quality and outcomes.

# 11.0 References


Ba, E. C. T. et al., 2022. Deconvolution Process Approach in Raman Spectra of DLC Coating to Determine the sp3 Hybridization Content Using the ID/IG Ratio in Relation to the Quantification Determined by X-Ray Photoelectron Spectroscopy. *Diamond and Related Materials.*

Brown, S. D., Tauler, R. & Walczak, B., 2009. *Comprehensive Chemometrics: Chemical and Biochemical Data Analysis.* Frisco, Colorado, USA: Elsevier.

Chen, H. et al., 2018. Eliminating Non-linear Raman Shift Displacement Between Spectrometers via Moving Window Fast Fourier Transform Cross-Correlation. *Frontiers in Chemistry,* pp. 1 - 11.

Ching, R., 2017. *Measuring Ash Content in Coal using Portable X-Ray Fluorescence,* Brandon, Canada: Brandon University.

Chirala, S. K. & Kumar , S. N., 1990. Area Normalization of the Renal Region of Interest in Radionuclide Renography Data Analysis: A Misconception. *International Journal of Radiation Applications and Instrumentation,* pp. 243 - 245.

Coal Services, 2023. *Test Report No. 23-0302/01 Roadwat Dust Analysis.* Thornton(NSW): Coal Services.

Czamara, K. et al., 2015. Raman Spectroscopy of Lipids: A Review. *Journal of Raman Spectroscopy,* pp. 4 - 20.

Devarakonda, N., Subhani, S. & Althaf, S., 2014. *Outliers Detection in Regression Analysis Using Partial Least Square Approach.* s.l., Springer, pp. 125 - 135.

Han, J., Kamber, M. & Pei, J., 2012. *Data Mining: Concepts and Techniques.* Waltham, Massachusetts, USA: Morgan Kaufmann.

Harris, M. L., Sapko, M. J., Varley, F. D. & Weiss, E. S., 2012. *Coal Dust Explosibility Meter Evaluation and Recommendations for Application,* Pittsburgh, Pennsylvania, USA: National Institute for Occupational Safety and Health.

Kasbekar, R. S., Ji, S., Clancy, E. A. & Goel, A., 2023. Optimizing the Input Feature Sets and Machine Learning Algorithms for Reliable and Accurate Estimation of Continuous, Cuffless Blood Pressure. *Nature Portfolio,* pp. 1-13.

Liu, Q. et al., 2023. Application of KM-SMOTE for Rockburst Intelligent Prediction. *Tunnelling and Underground Space Technology.*

NSW Resources Regulator, 2015. [Online] Available at: https://www.resourcesregulator.nsw.gov.au/sites/default/files/documents/nsw-code-of-practice-roadway-dust-analysis-in-underground-coal-mines.pdf

Qin, Y. et al., 2024. Deep Learning Analysis for Rapid Detection and Classification of Household Plastics Based on Raman Spectroscopy. *Spectrochimica Acta Part A: Molecular and Biomolecular Spectroscopy.*

Quirico, E., Rouzaud, J.-N., Bonal, L. & Montagnac, G., 2005. Maturation Grade of Coals as Revealed by Raman Spectroscopy: Progress and Problems. *Spectrochimica Acta Part A,* pp. 2368 - 2377.

Reaources Safety and Health Queensland, 2023. *Recongnised Standard 5.* [Online] Available at: https://www.rshq.qld.gov.au/__data/assets/pdf_file/0006/240378/recognised-standard-05.pdf

Sapko, M. J., Cashdollar, K. L., Green, G. M. & Verakis, H. C., n.d. *Coal Dust Particle Size Survey of U.S. Mines.* [Online] Available at: https://www.cdc.gov/niosh/mining/UserFiles/works/pdfs/cdpss.pdf

Schauenburg, 2023. *CDEM-1000 Coal Dust Explosibility Meter.* [Online] Available at: https://schauenburg-us.com/cdem/

Schmid, M., Rath, D. & Diebold, U., 2022. Why and How Savitzky–Golay Filters Should Be Replaced. *ACS Publications,* pp. 185-196.

Schwertman, N. C., Owens, M. A. & Adnan, R., 2004. A Simple More General bBoxplot Method for Identifying Outliers. *Computational Statistics & Data Analysis,* pp. 165 - 174.

Simtars, 2022. *Procedure for Determination of the Incombustible Content of Roadway Dust.* Mackay(QLD): Simtars.

Smith, E. & Dent, G., 2005. *Modern Raman Spectroscopy – A Practical Approach.* Chichester, England: John Wiley & Sons.

Vergara Sassarini, N. A. et al., 2023. Automatic Organofacies Identification by Means of Machine Learning on Raman Spectra. *International Journal of Coal Geology.*

Wedel, D. J., Belle, B. & Kizil, M. S., 2015. *The Effectiveness of Rapid Stone Dust Compliance Testing in Underground Coal.* Wollongong, NSW, Australia, The University of Wollongong, pp. 259 - 270.

Xu, J. et al., 2021. Raman Spectroscopy as a Versatile Tool for Investigating Thermochemical Processing of Coal, Biomass, and Wastes: Recent Advances and Future Perspectives. *Energy Fuels,* pp. 2870 - 2913.

# 12.0 Appendix

## 12.1. Spectrometer Selection

| Instrument Name | Sensor Type | Spectral Range | Price (AUD) | Chosen? | Excluded due to: |
|---|---|---|---|---|---|
| Stellarnet ADK NIR | InGaAs Photodiode array | 900-1700nm | ~$25,000 | Yes | N/A |
| Lightnovo | Raman | | | Yes | N/A |
| Ibsen PEBBLE | InGaAs Photodiode array | 950-1700nm | | No | High upfront development |
| Hamamatsu MEMS-FPI | InGaAs PIN photodiode with Fabry-Perot Interferometer (MEMS-FPI) | 1350-1650nm<br>1550-1850nm<br>1750-2150nm | ~$1000 for sensor<br>~$3000 for development kit | No | Lack of spectral sensitivity required for early demonstrator, high upfront development |
| Hamamatsu FT-IR engine | InGaAs PIN photodiode | 1100-2500 nm | ~$10,000 | No | High upfront development |
| Spectral Evolution NIR | | | ~$80,000 | No | Cost |
| Spectral Engine | | | ~$8,000 | No | Lack of spectral sensitivity required for early demonstrator |
| AMS AS7343 | Vis/NIR photodiode matrix | | ~$20 for sensor<br>~$800 for development kit | No | Lack of spectral sensitivity required for early demonstrator, High upfront development |
| AMS AS7421 | NIR photodiode matrix | | ~$35 for sensor<br>~$1200 for development kit | No | Lack of spectral sensitivity required for early demonstrator, very high upfront development |

## 12.2. Budget Breakdown

| Item | Cost (AUD ex GST) | Simtars | Coal Health and Safety Trust | Comment |
|---|---|---|---|---|
| Stellarnet NIR ADK | $23,515.00 | | 23,515.00 | |
| Lightnovo Raman Spectrometer | $20,643.00 | | 20,643.00 | |
| Laboratory Analysis | $12,157.00 | 6,902.50 | 5,418.50 | Internal and external laboratory analysis for coal quality and incombustible content |
| Sample Preparation | $4,459.00 | 3,095.00 | 1,364.00 | Labour only |
| Set-up and Testing | $16,881.00 | 12,601.00 | 4,280.00 | Labour and test setup |
| Analysis and Machine Learning | $16,485.00 | 11,794.50 | 4,690.50 | Labour only |
| Administration | $3,568.00 | $3,568.00 | | Labour only |
| **Total** | **$97,708.00** | **$37,961.00** | **$59,911.00** | |